Microscopie à force magnétique et microscopie tunnel polarisée en spin

André Thiaville

Laboratoire de Physique des Solides
Université Paris-Sud & CNRS, Orsay

coll. : José Miguel García, Jacques Miltat, Carole Vouille, François Caud

Plan

1 – Microscopie à force magnétique

principe
images de nanostructures
interprétation des images – modélisation

2 – Microscopie tunnel polarisée en spin

principe
modes courant et spectroscopie
quelques exemples de structures

Schéma de principe d'un AFM

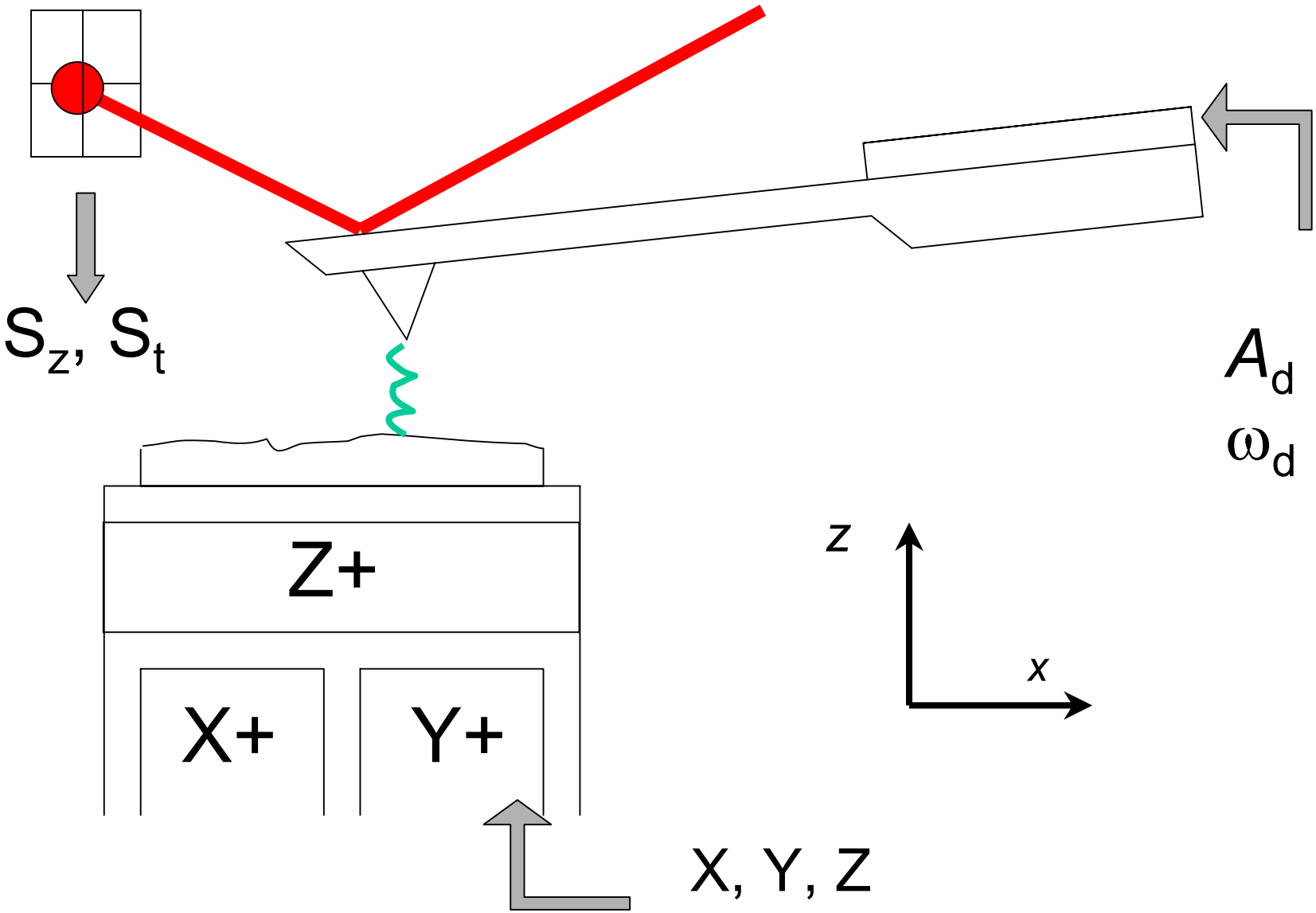

pointes

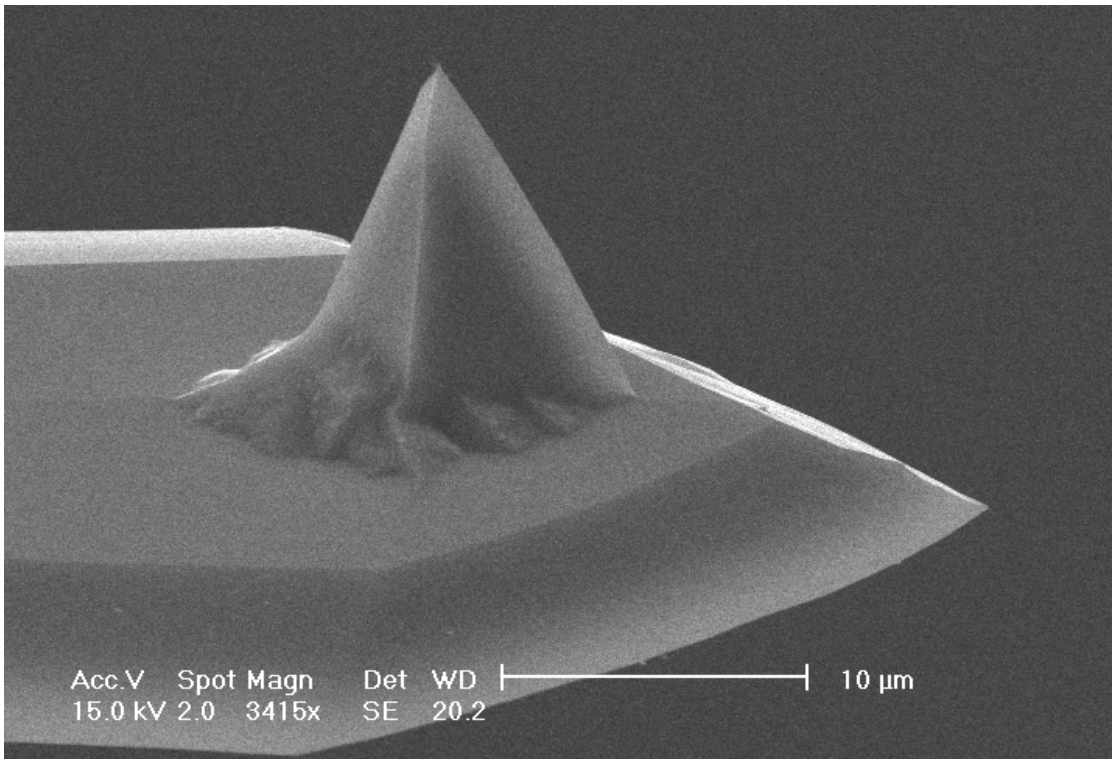

Si microfabriqué

f ~ 80 kHz (10-1000 kHz)
k ~ 5 N/m (0.1-100 N/m)
r ~ 20 nm

+ Dépôt par pulvérisation $Co_{80}Cr_{20}$
épaisseur = 5-30 nm

forces magnétiques

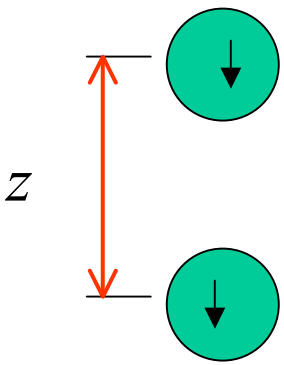

aimantation M_s
volume V

$$F_z = \frac{3\mu_0}{2\pi}\frac{(M_s V)^2}{z^4}$$

$M_s = 10^6$ A/m, $V = (10\ \text{nm})^3$, $z = 30$ nm

$F_z = 0.7$ pN

$$\frac{dF_z}{dz} = 4\frac{F_z}{z}$$

$dF_z/dz = 10^{-4}$ N/m

mécanique du levier

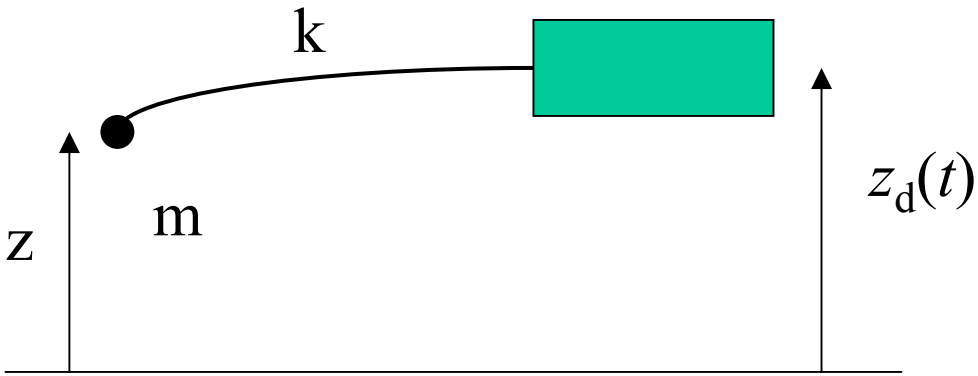

$$m\frac{d^2z}{dt^2} = F - k\left(z - z_d\right) - mb\frac{dz}{dt}$$

$$\omega_0 = \sqrt{k/m} \qquad b = \omega_0 / Q$$

statique : $\boxed{z = z_d + F/k}$

vibrant : $z_d = A_d \cos(\omega t) \rightarrow z = A\cos(\omega t + \varphi)$

F=0

$$A = \frac{A_d}{\sqrt{\left(1 - \omega^2/\omega_0^2\right)^2 + \left(\omega / Q\omega_0\right)^2}} \qquad tg\varphi = \frac{\omega\omega_0}{Q\left(\omega_0^2 - \omega^2\right)}$$

mécanique du levier (2)

vibrant : $F \neq 0$

$$F = F_0 + z\frac{dF}{dz} + \ldots$$

$$\omega_r = \sqrt{\frac{k - dF/dz}{m}}$$

$$\boxed{\frac{\Delta f}{f} = -\frac{1}{2k}\frac{dF}{dz}}$$

$$\boxed{\Delta\varphi = \frac{Q}{k}\frac{dF}{dz}}$$

Valeurs numériques (k=1 N/m, Q=100)

Δz= 0.7 pm ; $\Delta f/f$ = 5 10^{-5} ou $\Delta\varphi$=0.6°

thermodynamique du levier

agitation thermique ≡ force aléatoire à spectre blanc

$$< \Delta_{th} F >= \sqrt{\frac{4 k_B T\, kB}{\omega_0 Q}} \qquad < \Delta_{th} \frac{dF}{dz} >= \frac{< \Delta_{th} F >}{A}$$

B : bande passante de mesure = 4π x f_{ligne} x Nb pixels

Valeurs numériques

(f_0= 100 kHz, Q= 100, k=1 N/m, f_{ligne}=0.1 Hz, 100 pix, A= 10 nm)

$\Delta_{\text{th}} F = 2\ 10^{-13}$ N ; $\Delta_{\text{th}}\, dF/dz = 2\ 10^{-5}$ N/m

contrastes magnétique et topographique

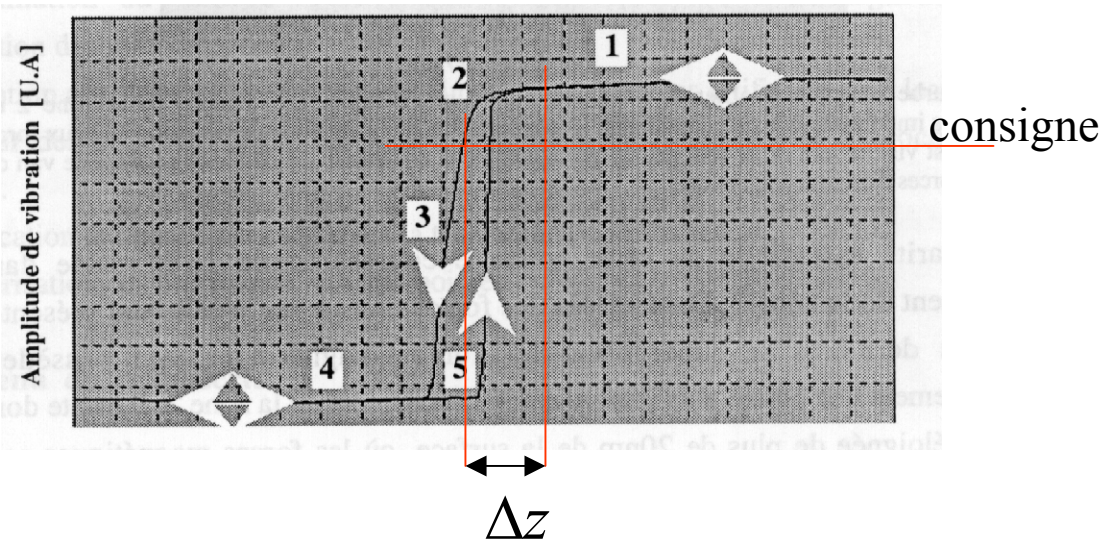

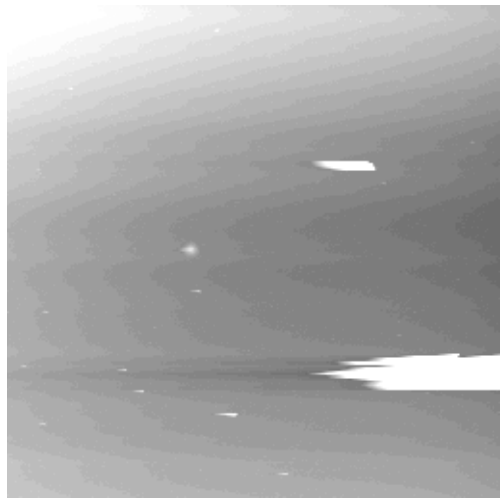

topo

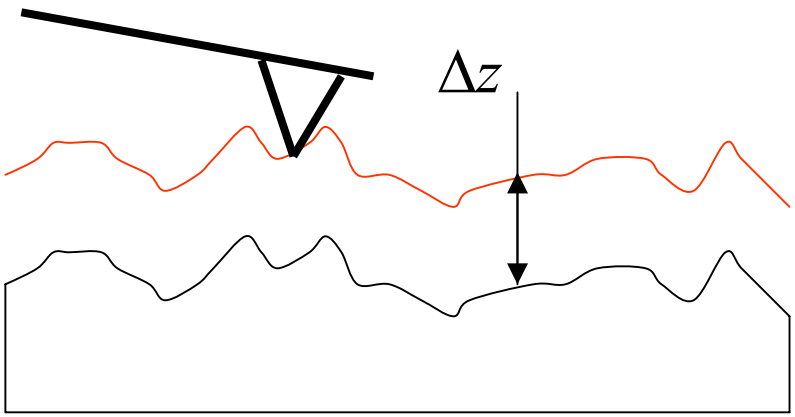

« lift mode »

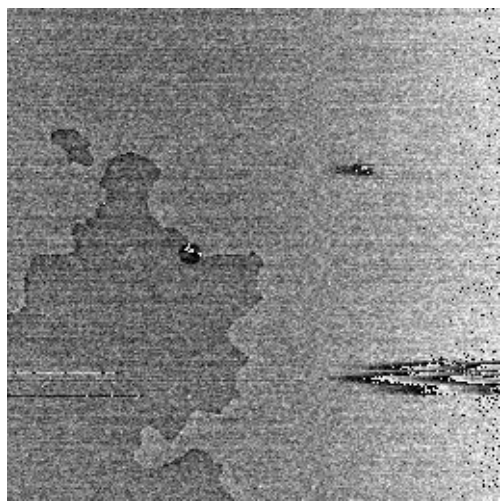

magn

Le MFM comme microscope de charges magnétiques

énergie d'interaction pointe-échantillon

$$E_{\text{int}} = -\mu_0 \int_{tip} \vec{M}_{tip} \cdot \vec{H}_{sample} = -\mu_0 \int_{sample} \vec{M}_{sample} \cdot \vec{H}_{tip}$$

le champ de l'échantillon dérive de ses charges

$$div\vec{H}_{sample} = \underbrace{-div\vec{M}_{sample}}_{\rho_{sample}} \quad \text{intérieur}$$

$$0 \quad \text{extérieur}$$

$$\vec{H}_{sample} \cdot \vec{n}\Big|_{out} = \vec{H}_{sample} \cdot \vec{n}\Big|_{in} + \underbrace{\vec{M}_{sample} \cdot \vec{n}}_{\sigma_{sample}}$$

$$\boxed{E_{\text{int}} = \iint_{sample} \sigma_{sample} \phi_{tip} + \iiint_{sample} \rho_{sample} \phi_{tip}}$$

$$\vec{H}_{tip} = -\overrightarrow{grad}\phi_{tip}$$

ϕ_{tip} **potentiel de la pointe**

A. Hubert, W. Rave, S.L. Tomlinson, phys. stat. sol. **(b)204** 817 (1997)

Petits éléments de permalloy

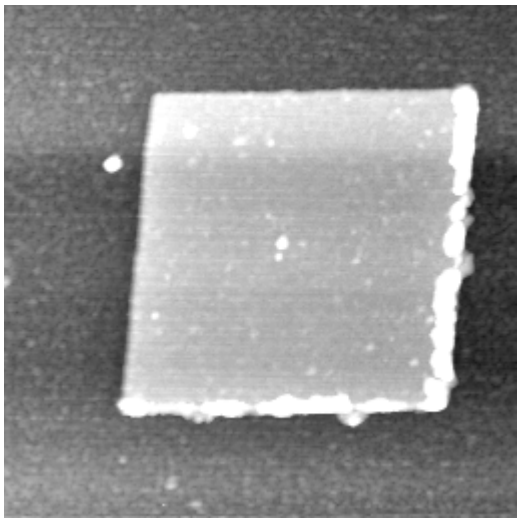

Topographie
2µmx2µm

(épaisseur 16 nm)

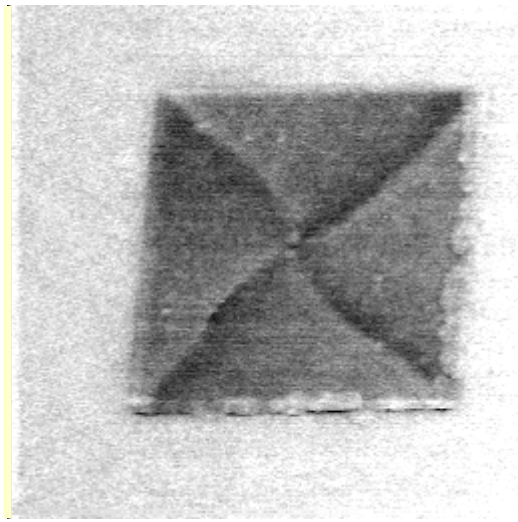

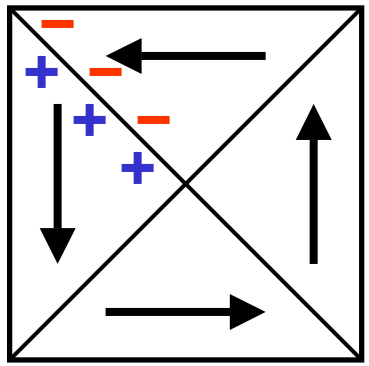

structure de type
Landau

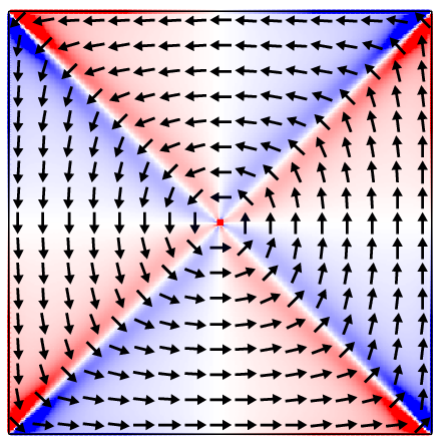

charges
magnétiques

J.M. Garcia et al.,
Appl. Phys. Lett. **79** 656 (2001)

Parois en cross-tie

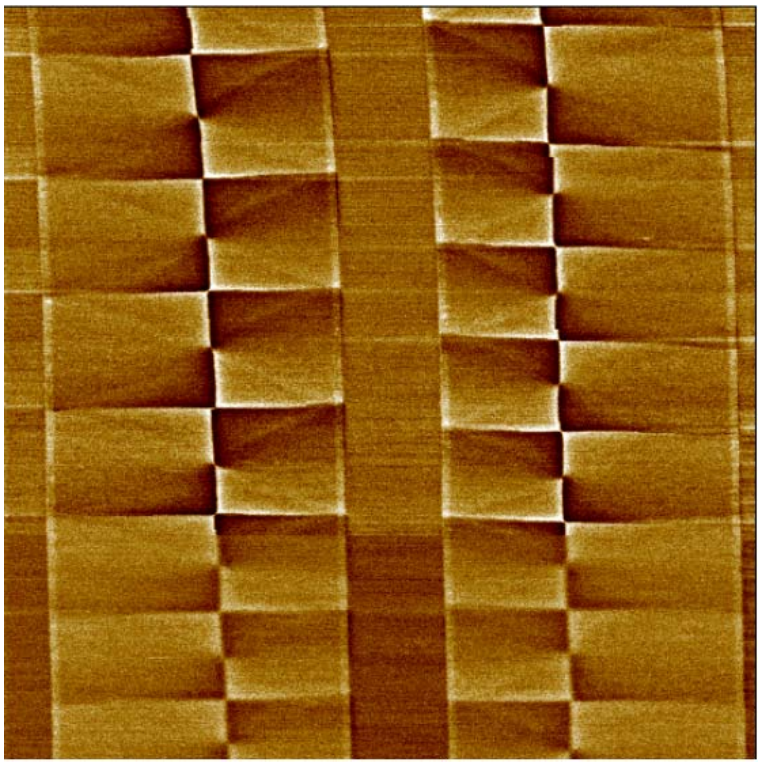

12 µm

2 bandes de permalloy
(épaisseur 35 nm)

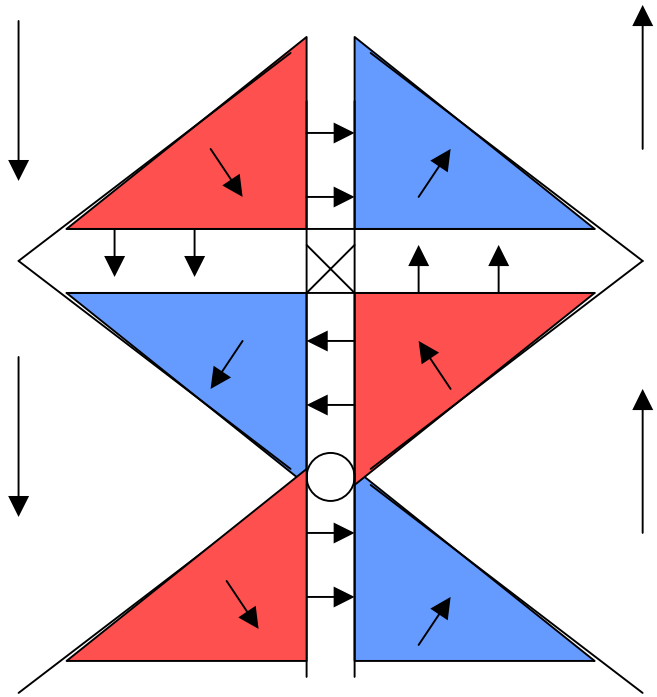

H. Joisten et al.
J. Magn. Magn. Mater.
233 230 (2001)

COBALT CYLINDERS PATTERNED BY INTERFERENCE LITHOGRAPHY

(A. Fernandez et al. IEEE Trans. Magn. 32 4472 (1996))

diam 100 nm
height 40 nm

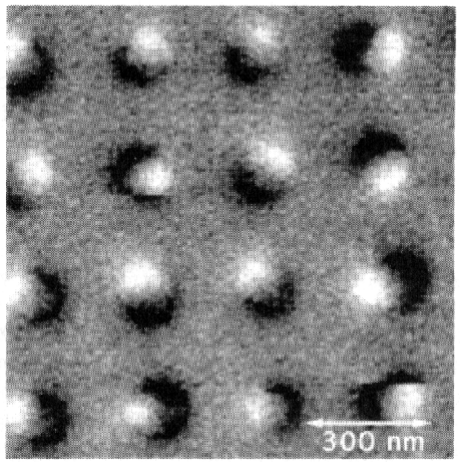

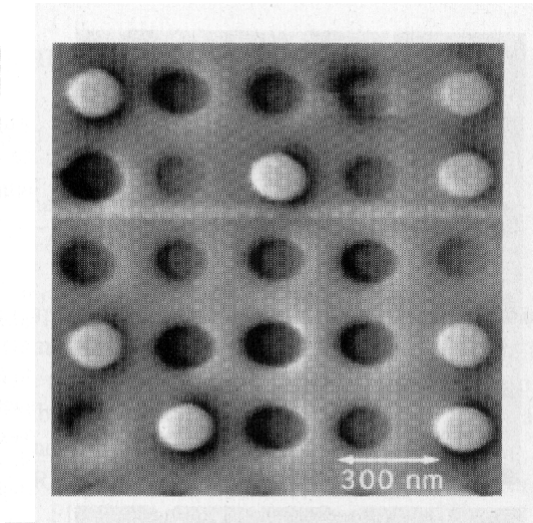

diam 70 nm
height 100 nm

In plane magnetization

Perpendicular magnetization

Effect of the aspect ratio of the cylinder

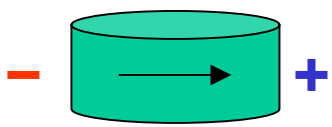

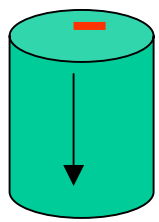

MFM of magnetic dots in a vortex state

First observation: T. Shinjo et al., Science **289** (2000) 930

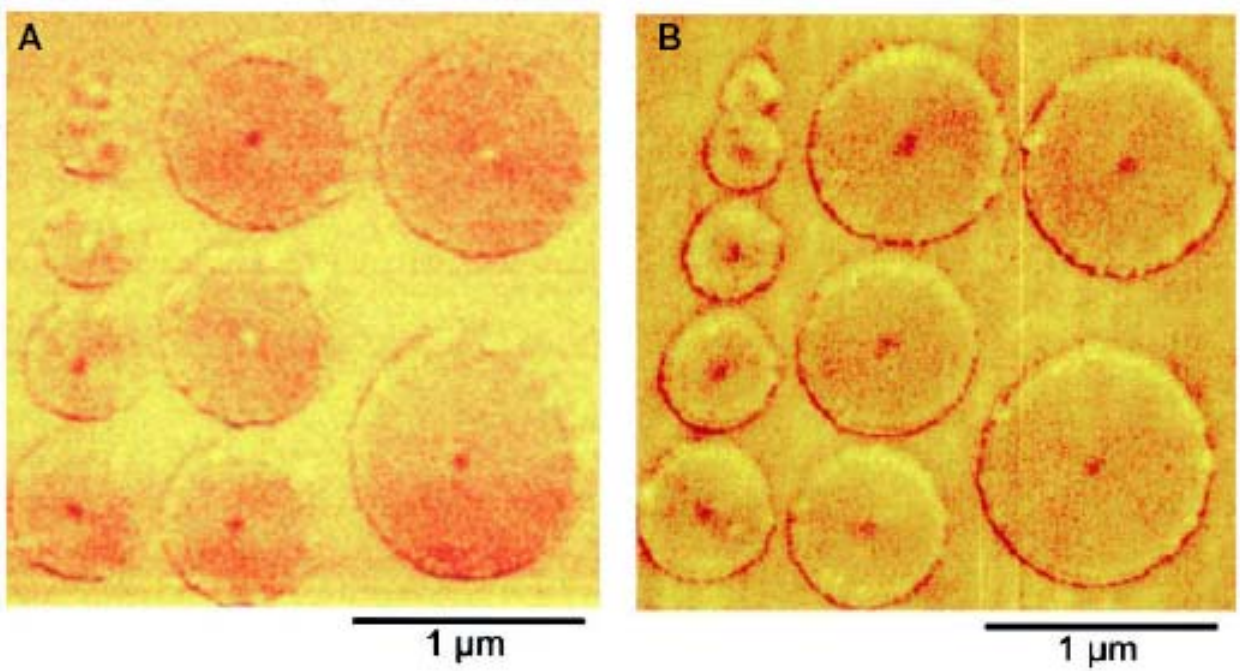

Natural state After saturation under 1 T

Sample : permalloy, 50 nm thick

MFM of a thicker square element

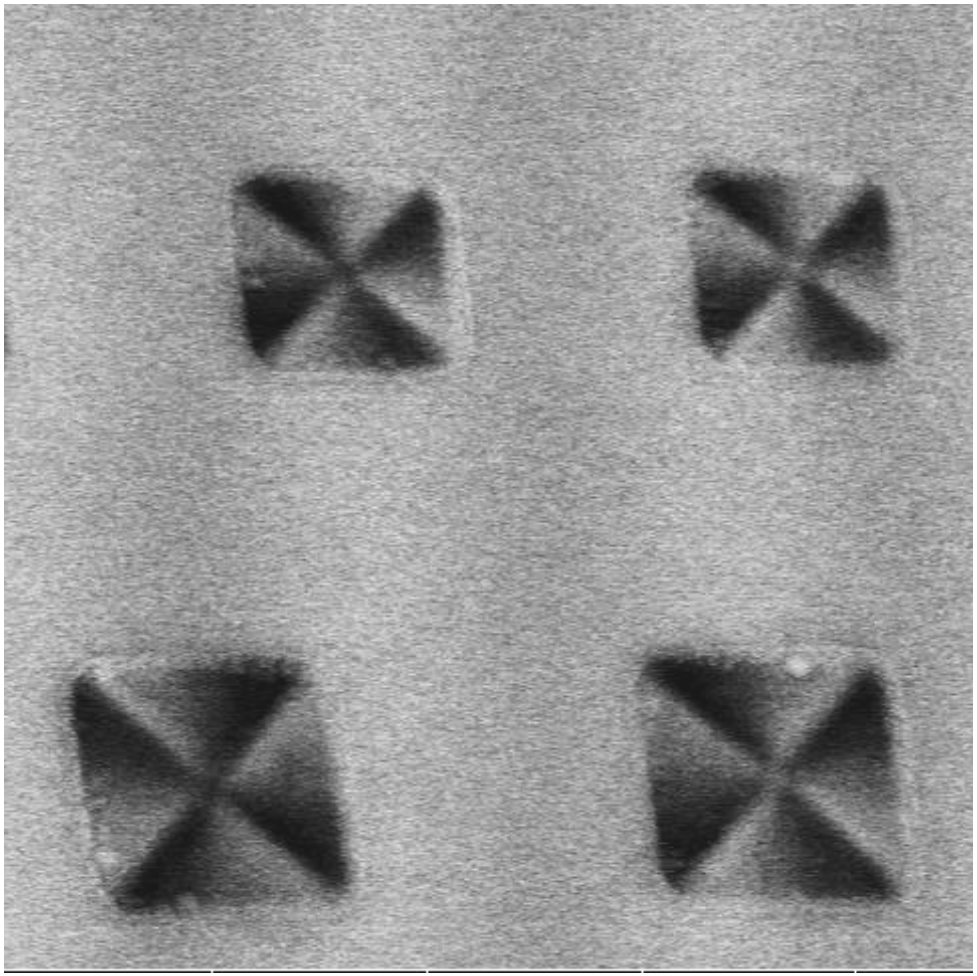

0.8 and 1 μm wide squares, 50 nm thick

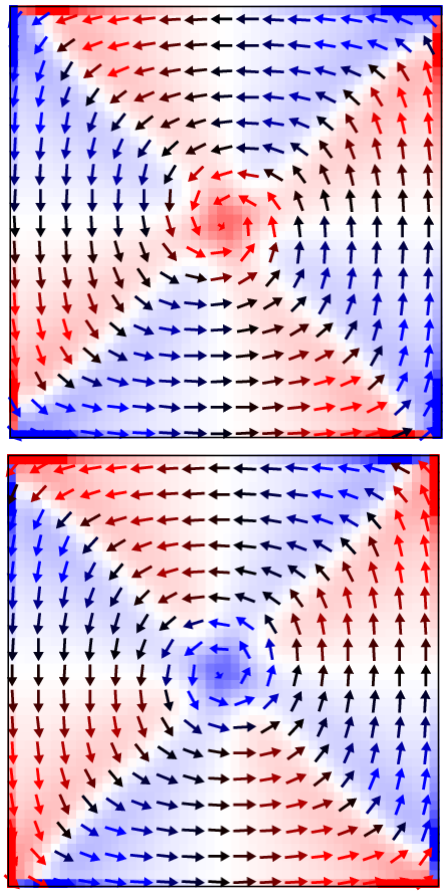

200 x 50 nm squares
Charges at top surface
for opposite cores

MFM sur des couches ultraminces de cobalt à aimantation perpendiculaire

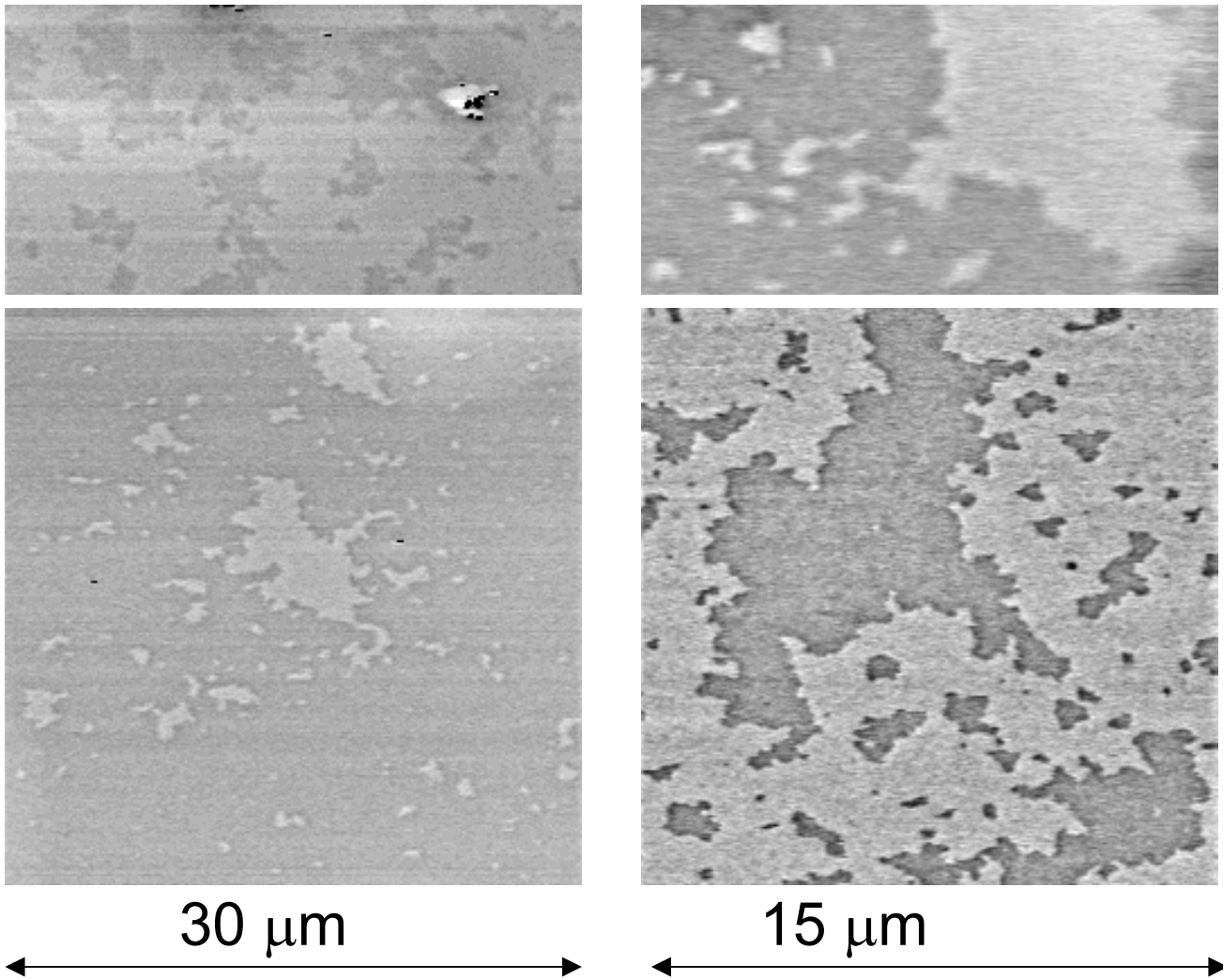

Au/ Co/ Au

13.9 Å

L. Belliard,
Ph.D. thesis
Orsay (1997)

Au delà de la microscopie de charges

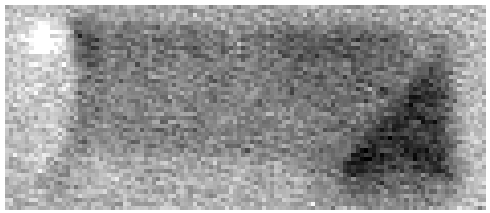

2 µm

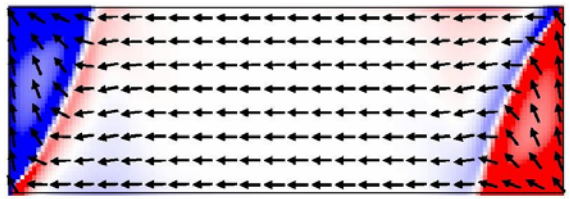

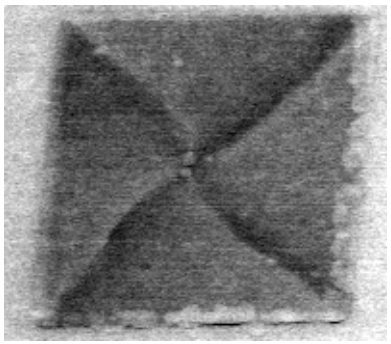

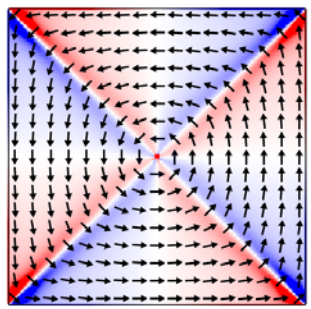

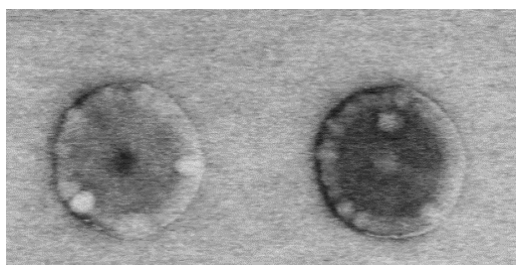

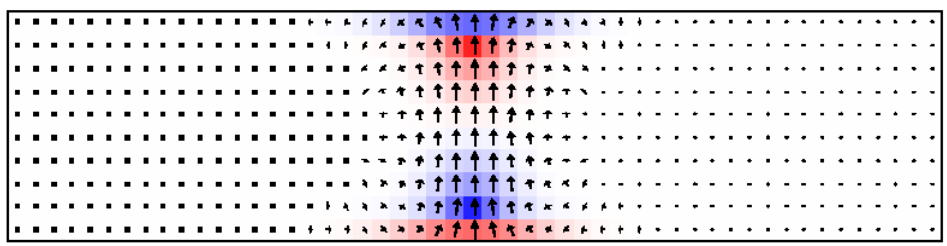

(coupe)

Perturbations dues au champ de la pointe

trace ▶ ◀ retrace

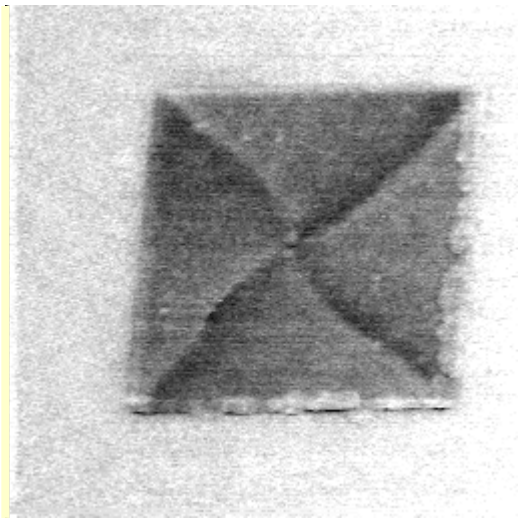

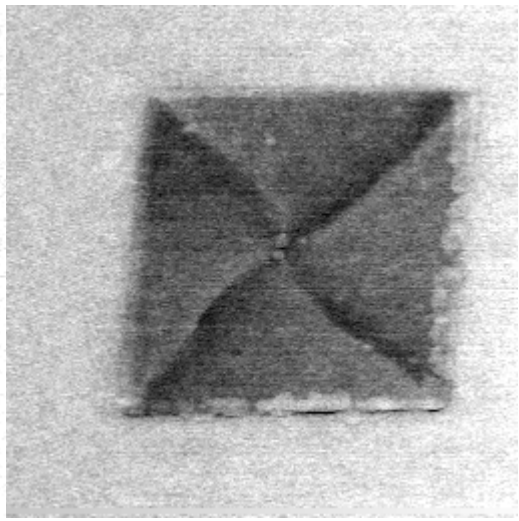

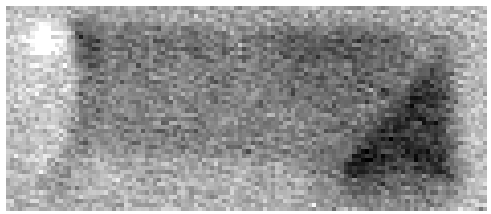

M_{pointe}:

z=20nm

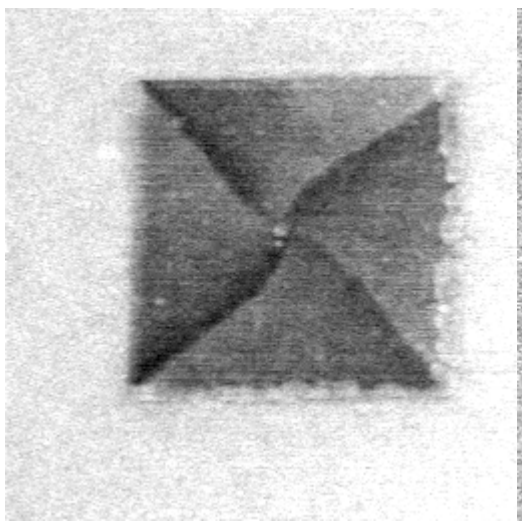

z=45nm

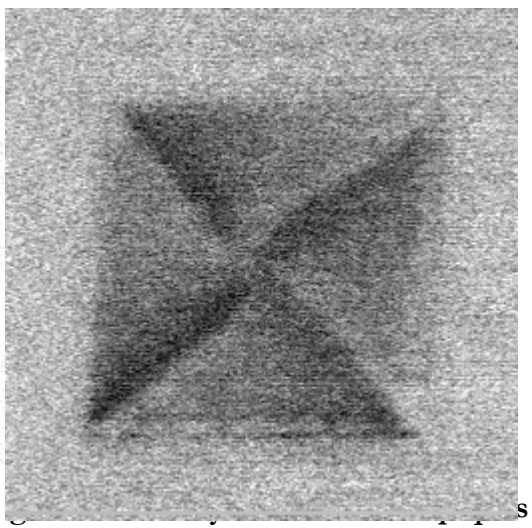

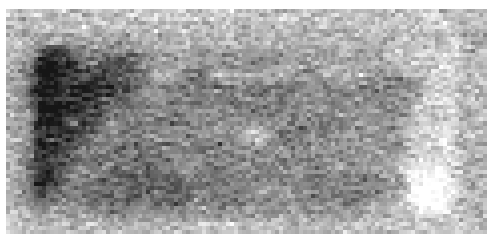

MFM: contrast simulation

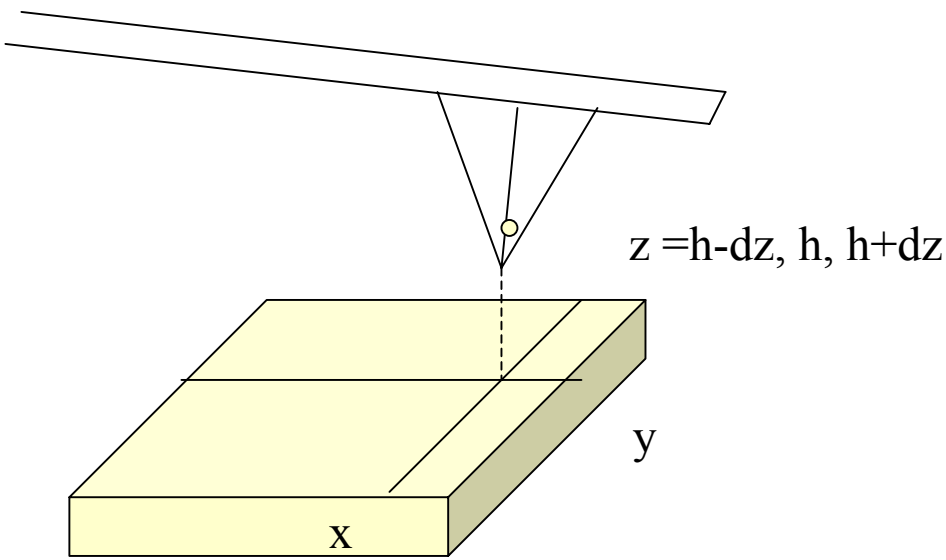

Micromagnetic simulation of the sample structure under the action of the tip field, for all positions of the tip (x, y, and z)

Assumption : fixed tip field and tip configuration

How can one compute the force between tip and sample ?

MFM: contrast simulation

First approach

(S. Tomlinson, e.g.
J. Magn. Magn. Mater.
161 385 (1996))

$$E_{\text{int}} = -\mu_0 \int_{tip} \vec{M}_{tip} \cdot \vec{H}_{sample} = -\mu_0 \int_{sample} \vec{M}_{sample} \cdot \vec{H}_{tip}$$

Use the values for the sample submitted to the tip field

Second approach

The system « tip + sample » is isolated

$$E_{tip} + E_{sample} + E_{int} + E_{elastic} = Constant$$

Constant
(hard tip)

$$F_{elastic} = -kz = \frac{\partial}{\partial z}\left(E_{sample} + E_{interaction}\right) = \frac{\partial}{\partial z}\left(E_{micromagnetic}\right)$$

$$-\frac{dF}{dz} = \frac{d^2E}{dz^2} \approx \frac{E(h+dz) + E(h-dz) - 2E(h)}{(dz)^2}$$

the MFM tip as a monopole

Results from a ***finite element*** tip micromagnetic model considering a conical shell of CoCr (F. Alouges, Orsay)

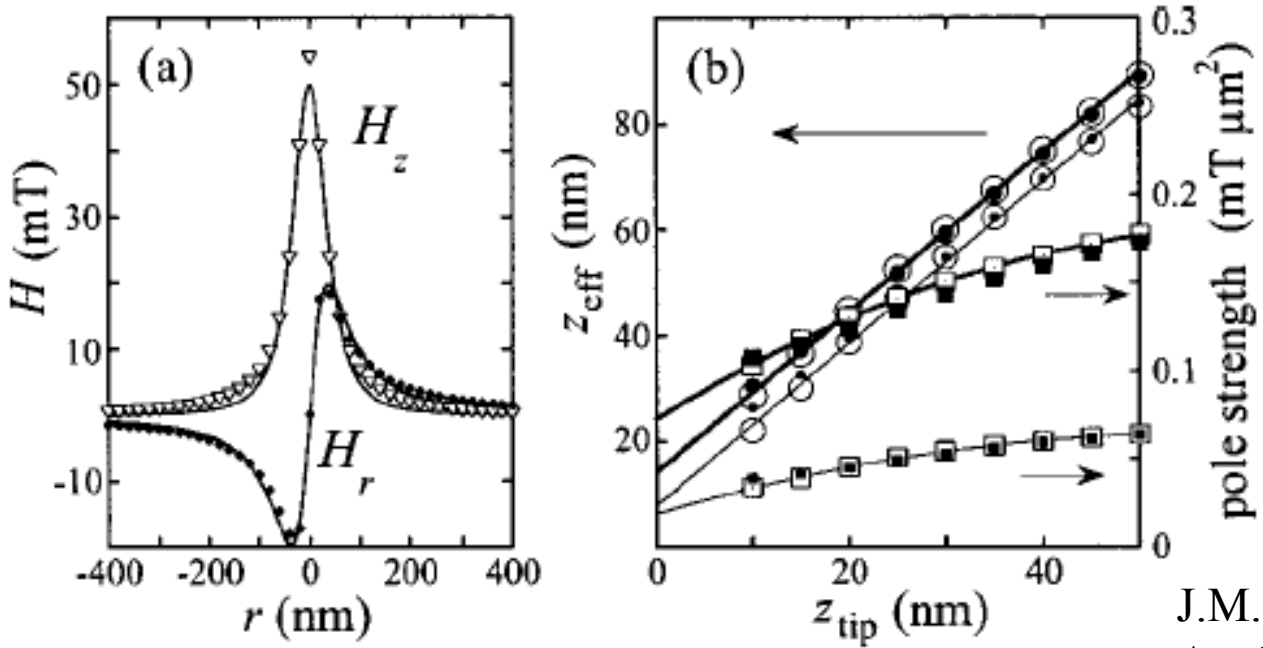

Large symbols:
20 nm thickness

Small symbols:
10 nm thickness

J.M. Garcia et al.,
Appl. Phys. Lett. **79** 656 (2001)

Monopole field fit → ***monopole strength*** and ***effective monopole height***

NB : there exist more complex tip models (extended charge model)
S. McVitie et al., J. Appl. Phys. **89** 3556 (2001)

PERTURBATION OF THE MAGNETIC STRUCTURE IN A NiFe SQUARE (1 μm) BY A MFM TIP

Negative monopole tip

Positive monopole tip

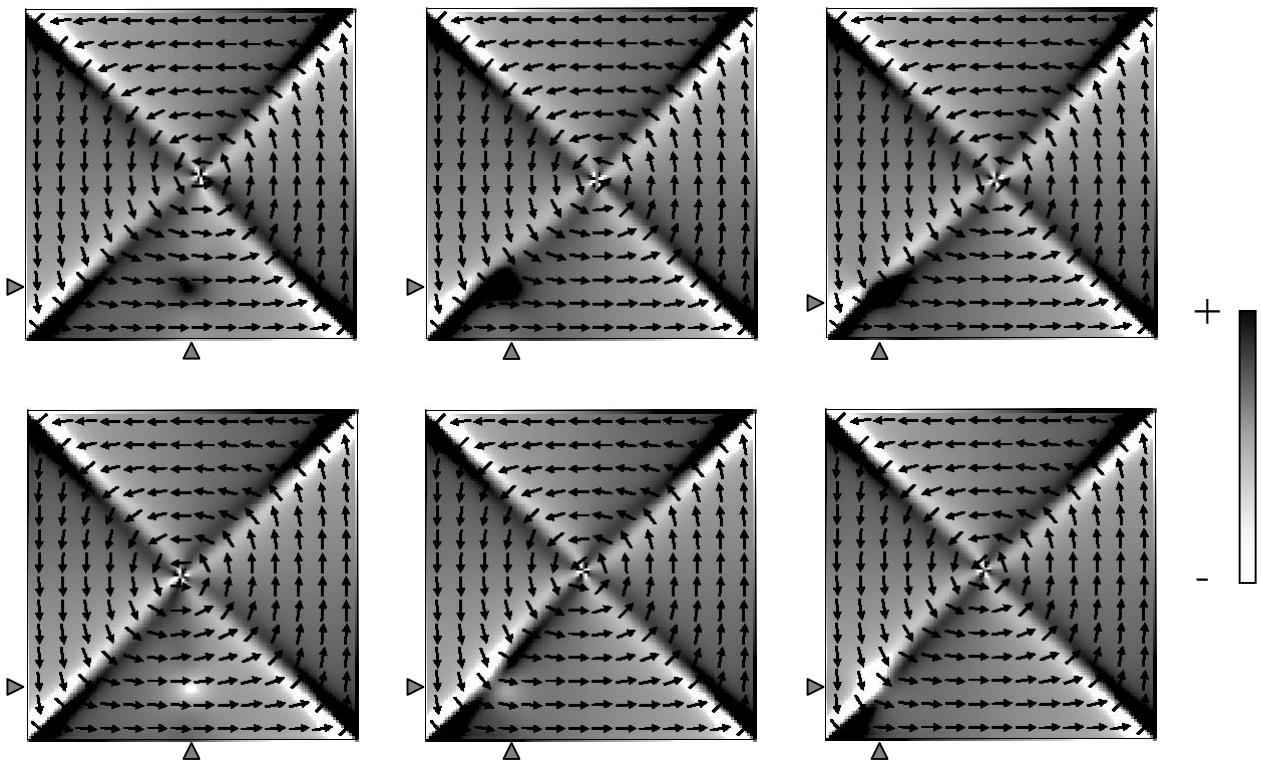

Color code : the magnetic charges div(m)

Monopole height : 60 nm above film top (16 nm film)
Maximum field at film center : 400 Oe

Image simulation results

Experimental Image

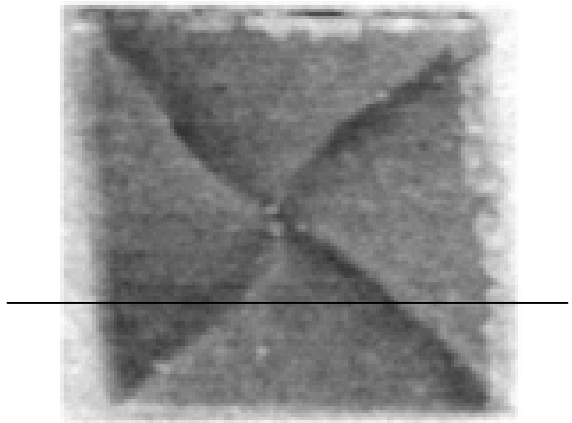

Simulated Image

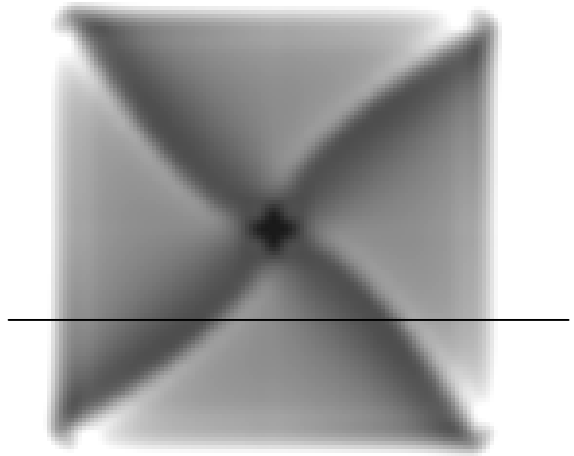

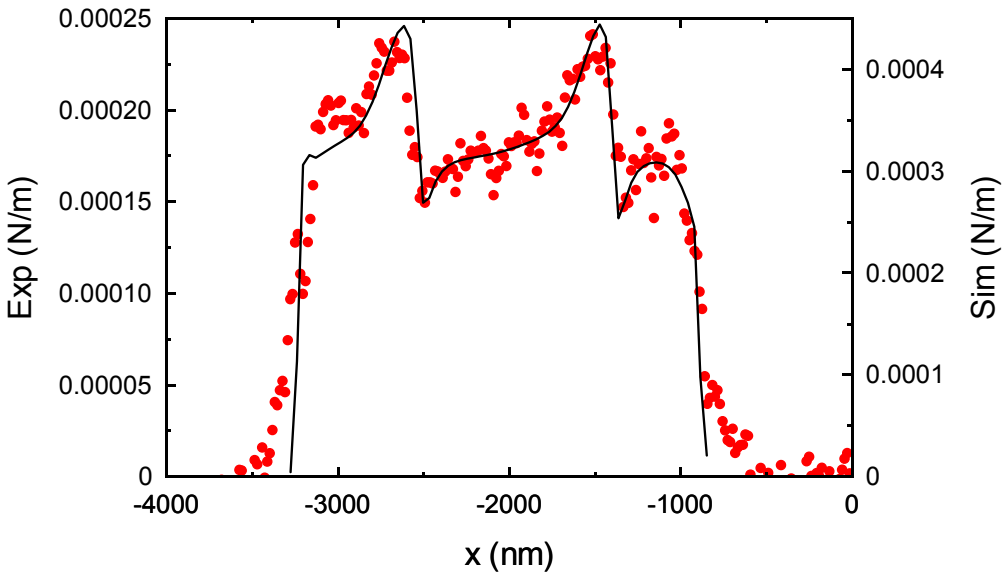

J.M. Garcia et al.,
Appl. Phys. Lett. **79** 656 (2001)

Comparison of three models

Experiments *versus* Simulations for square elements (size: 2 microns, thickness 16 nm)

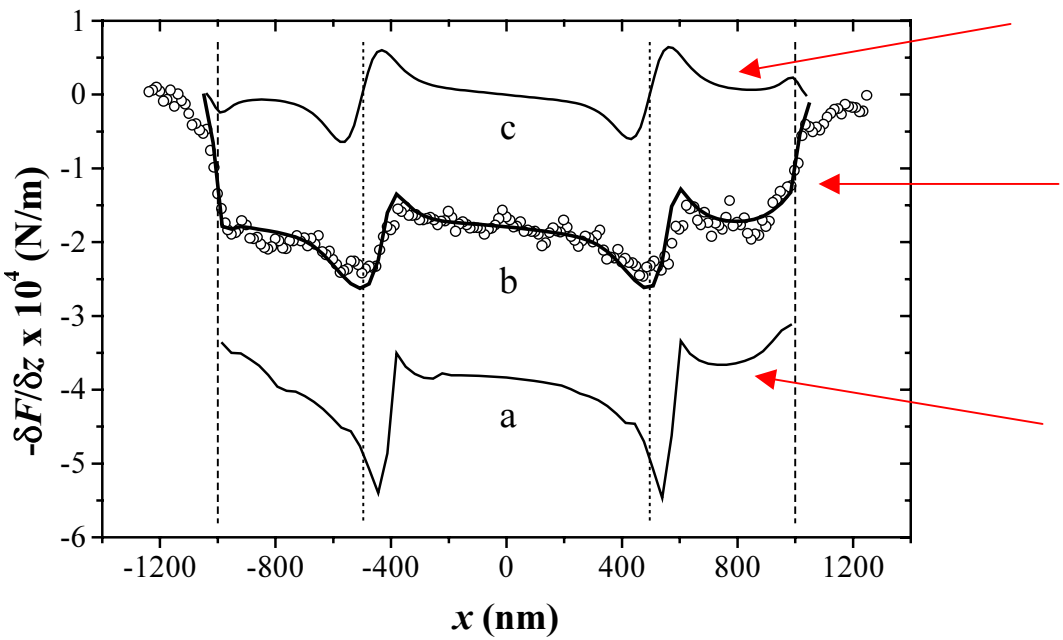

No perturbation model

Experiment (dots) and total energy calculation

Force from only the Zeeman energy term

J.M. Garcia et al. Appl. Phys. Lett. **79** 656 (2001)

MFM of a rectangular element

Experiments *versus* Simulations for rectangular elements (2.1 x 0.7 microns)

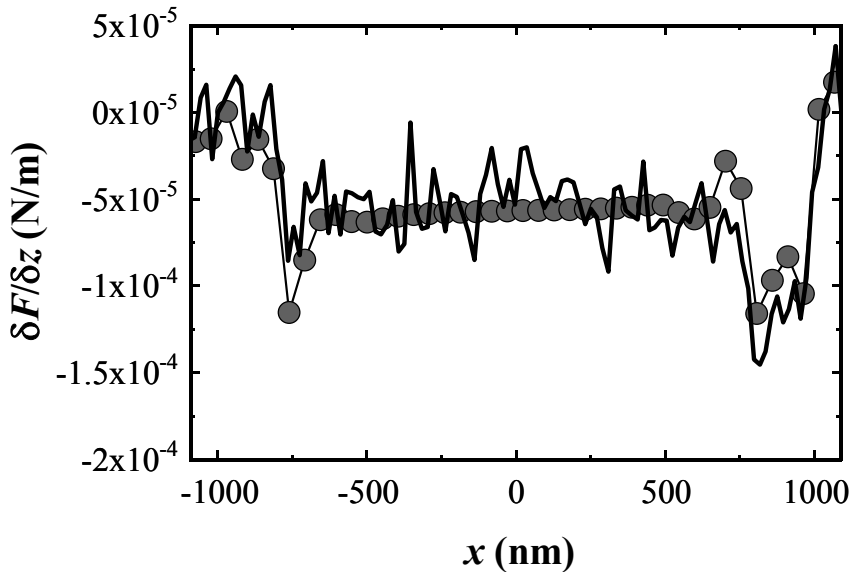

Experiment (curve) and
total energy calculation (dots)

J.M. Garcia et al.,
JMMM **249** 163 (2002)

Experimental image

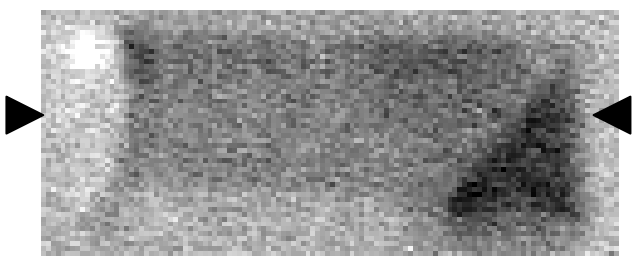

Color scale: Δω

Simulated image

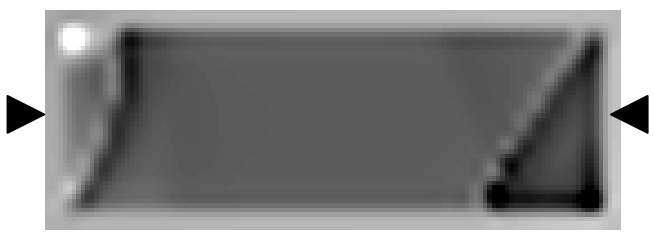

Color scale: - ∂F/∂z

MFM of magnetic dots in a vortex state

Careful selection of the tip moment

Image quality

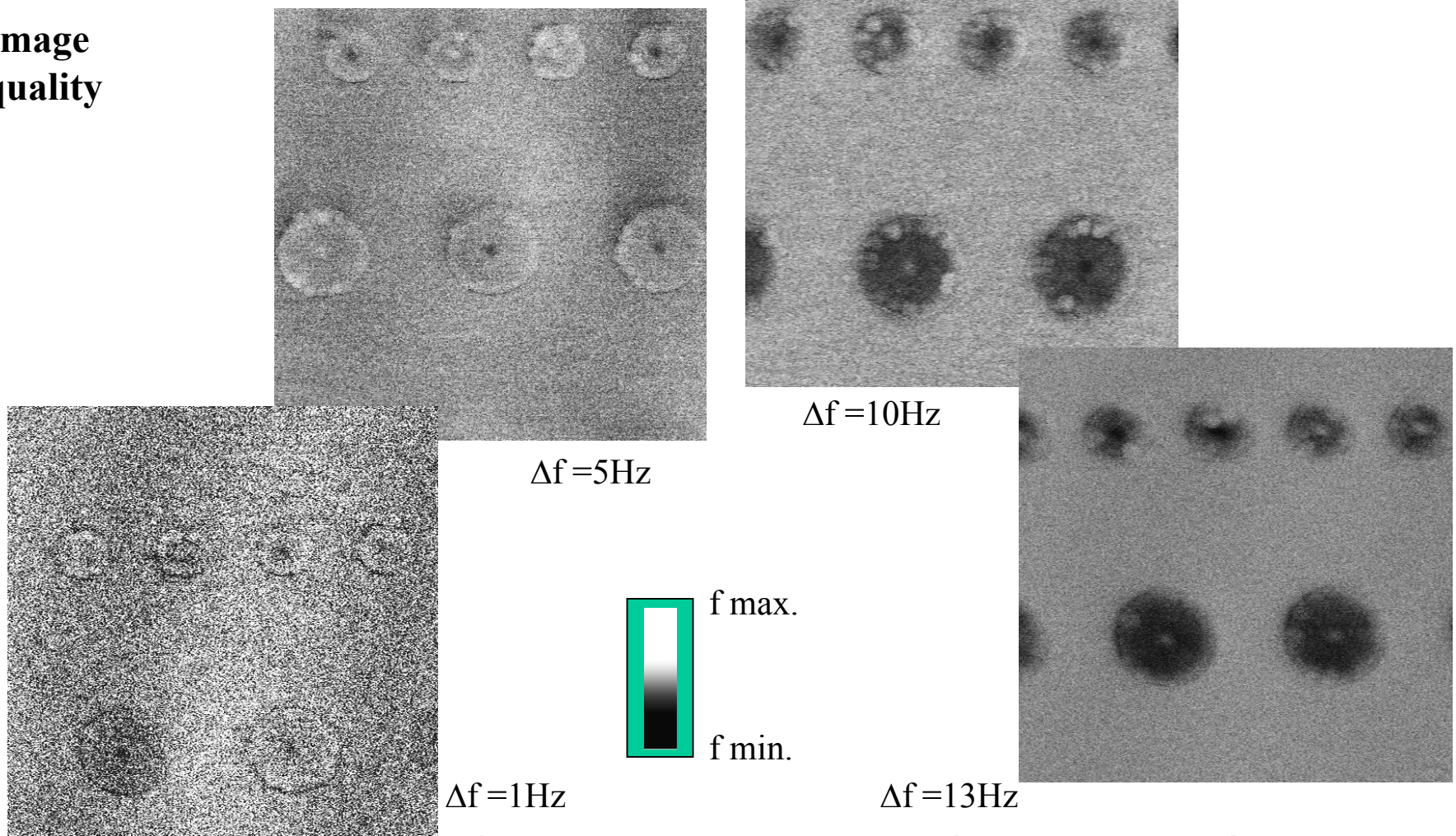

CoCr thickness (nm)

Contrast radial profiles : role of sample diameter

The global attraction by the sample increases with its diameter

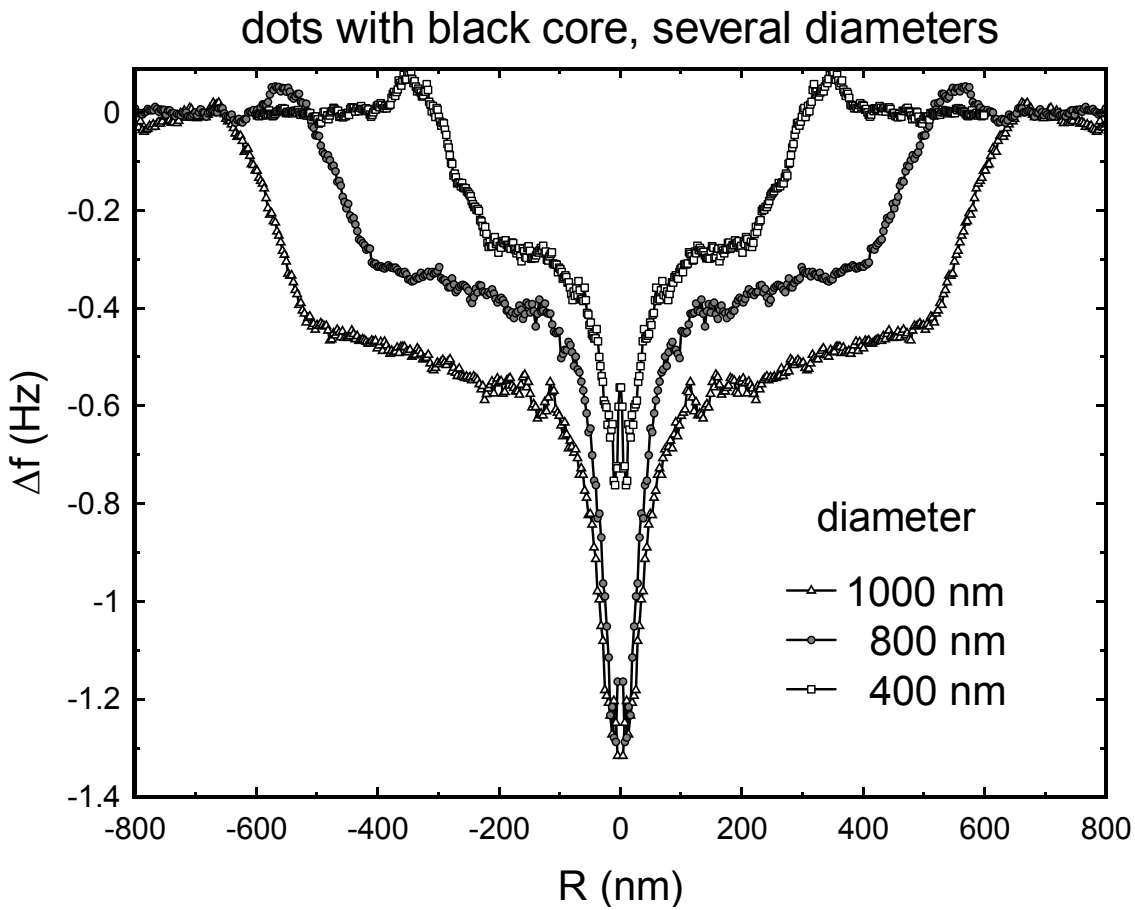

Model of Saenz, Garcia & Slonczewski

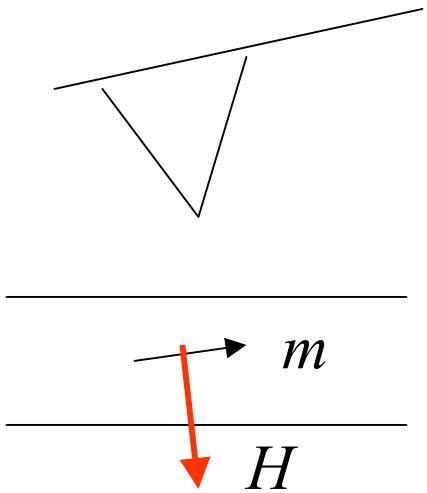

local response : $dm = \chi H_{perp}$

$$E_{int} = - \chi H^2_{perp}/2$$

Attraction of the magnetic tip by any magnetic sample

J.J. Saenz, N. Garcia, J.C. Slonczewski
Appl. Phys. Lett. **53** 1449 (1988)

Contrast radial profiles : role of the tip

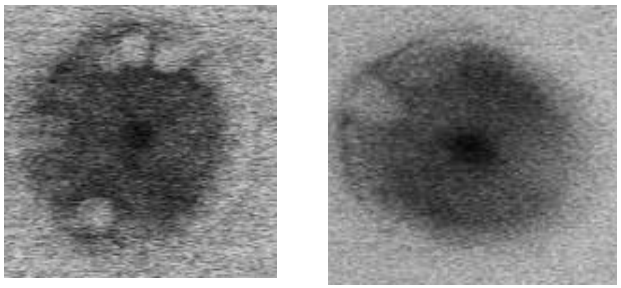

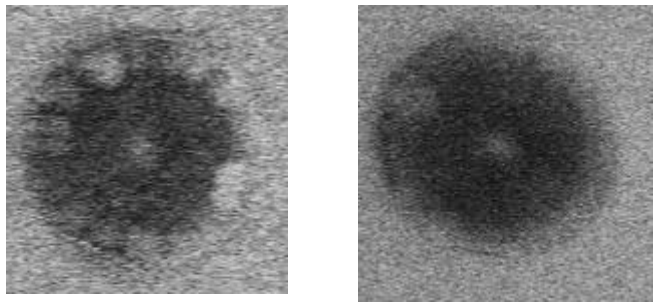

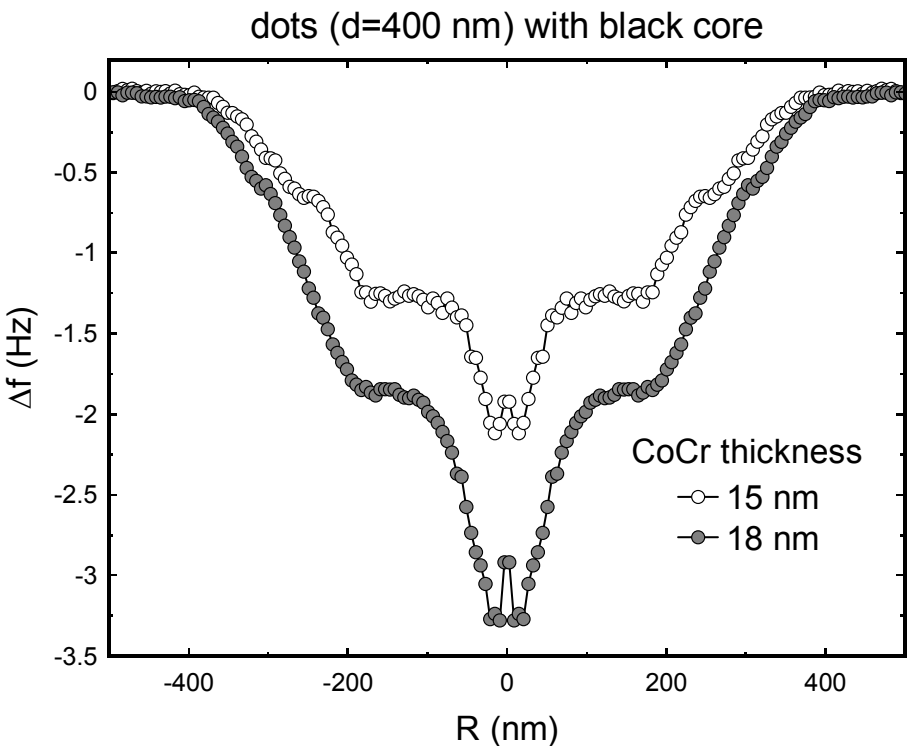

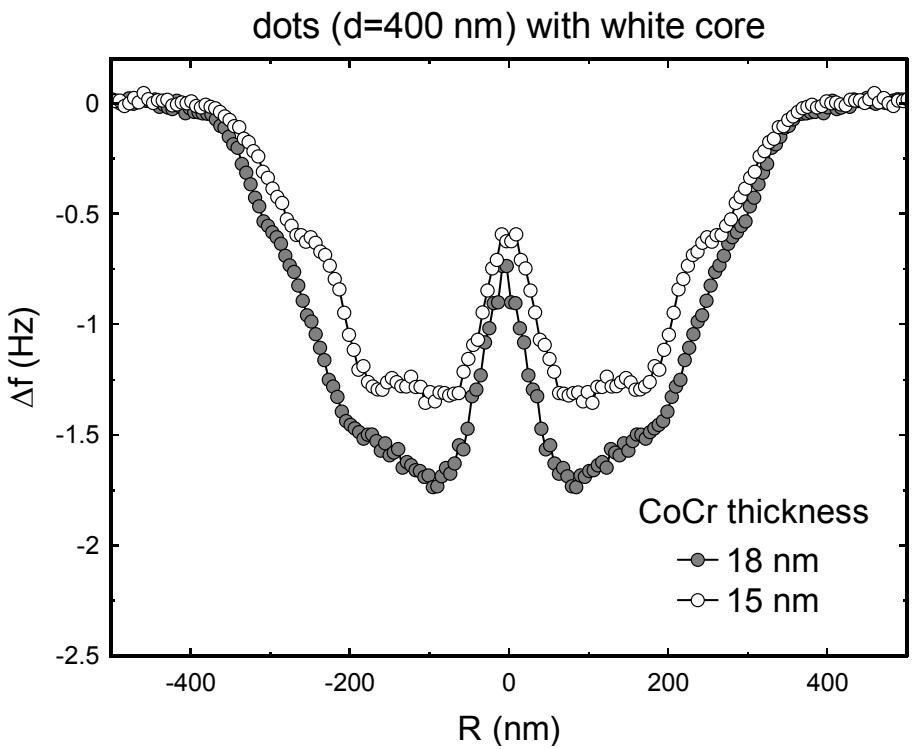

MFM: micromagnetic simulations

Magnetic charges at the sample top surface while the tip scans a half-diagonal

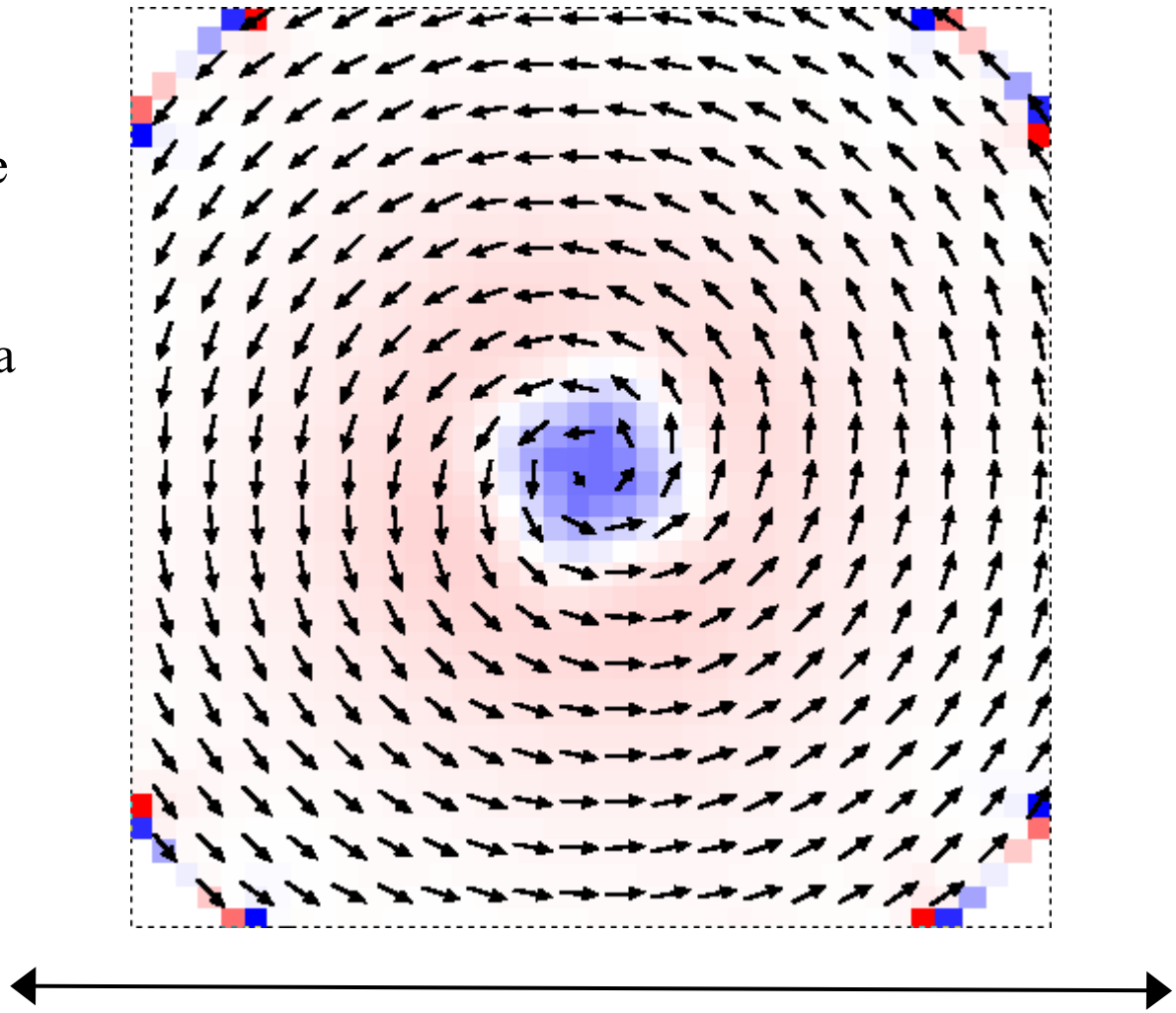

200 nm

MFM: experiments vs. simulations

Tip: CoCr thickness = 15 nm
Lift height = 20 nm
Frequency = 75 kHz

Monopole strength = 0.098 mT μm^2
Height above sample midplane = 65 nm
Δz = 5 nm

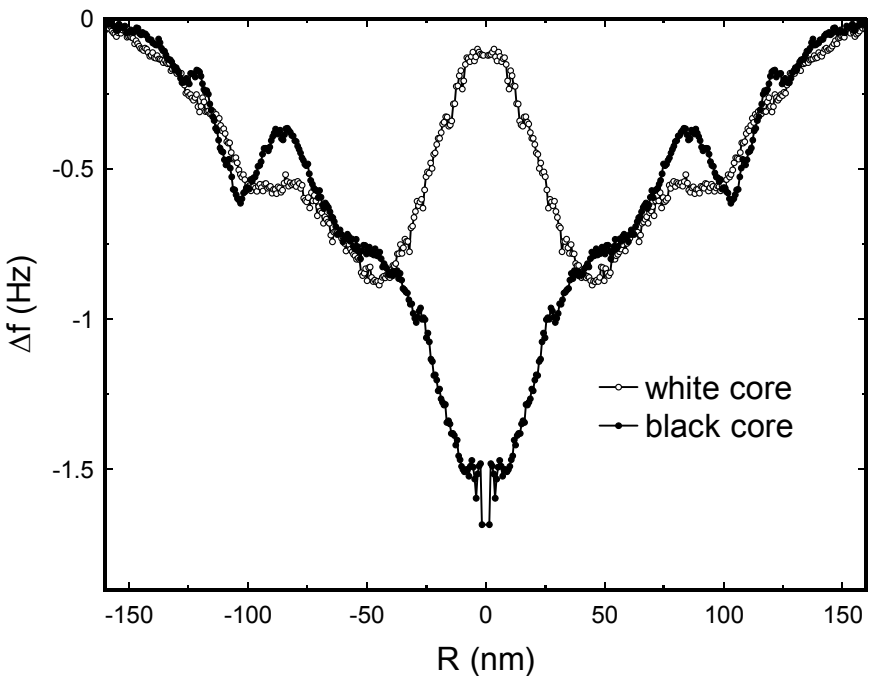

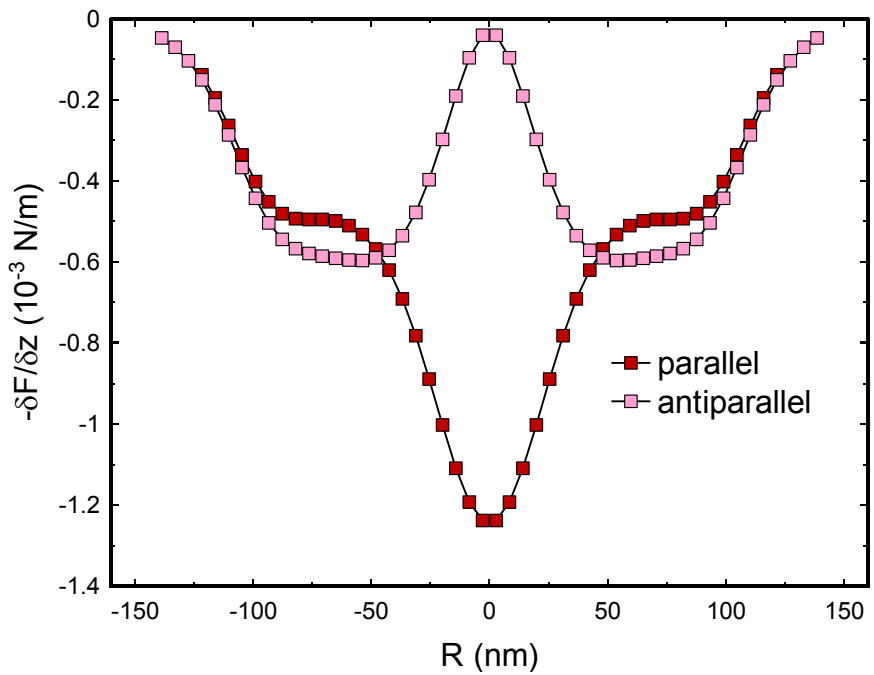

Sample : 200 nm diameter, 50 nm thickness, permalloy

MFM : experiments vs. simulations

200 nm diameter

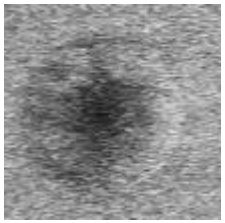

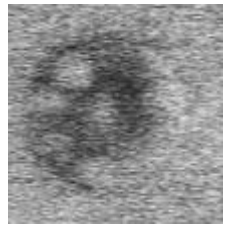

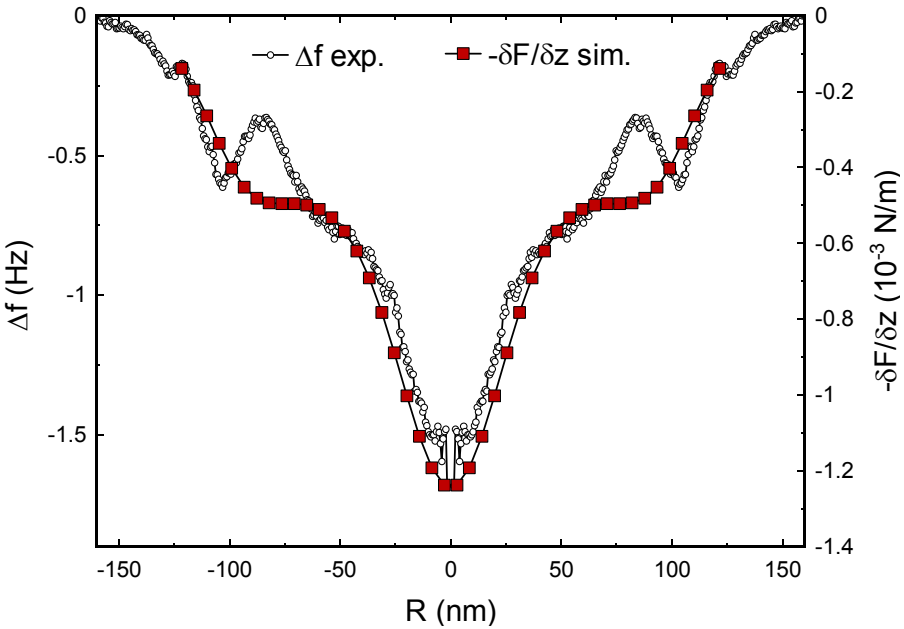

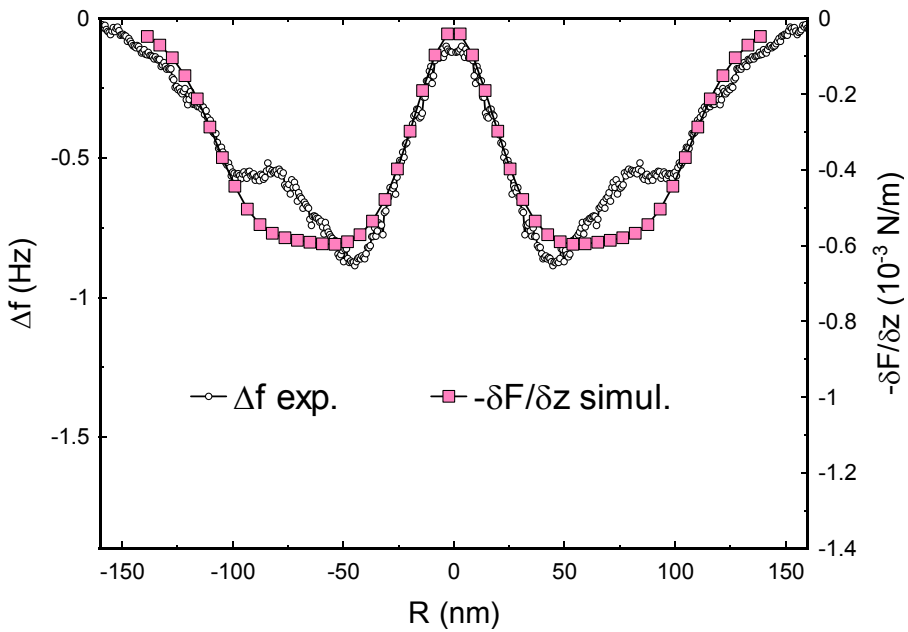

One problem: the transformation $\delta F/\delta z \rightarrow \Delta f_{sim} \approx \Delta f_{exp}$ requires too large k (but tip too close)

Comparison to other models : no perturbation case

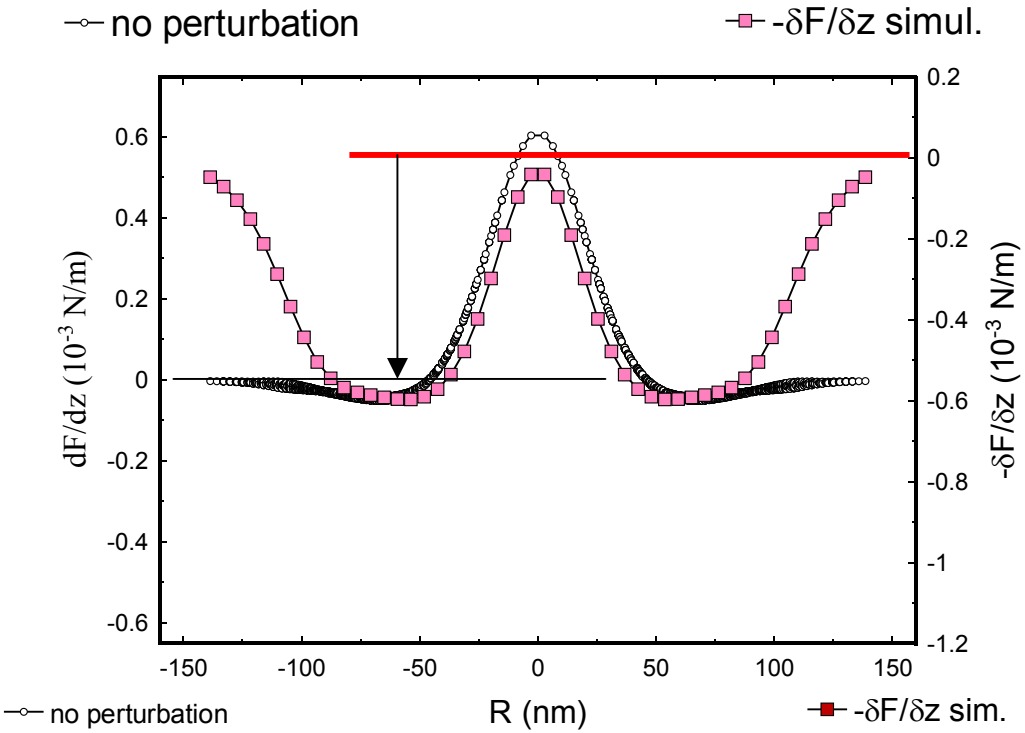

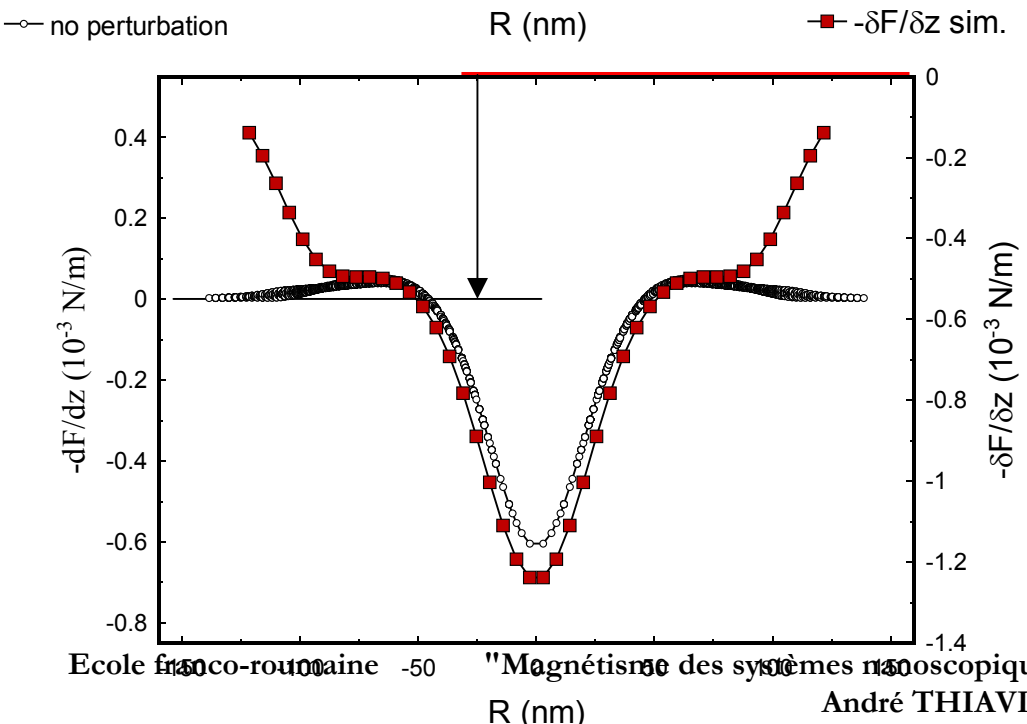

Without perturbation

- no overall attraction outside the core
- no asymmetry in core image intensity and width

Comparison to other models : interaction energy only

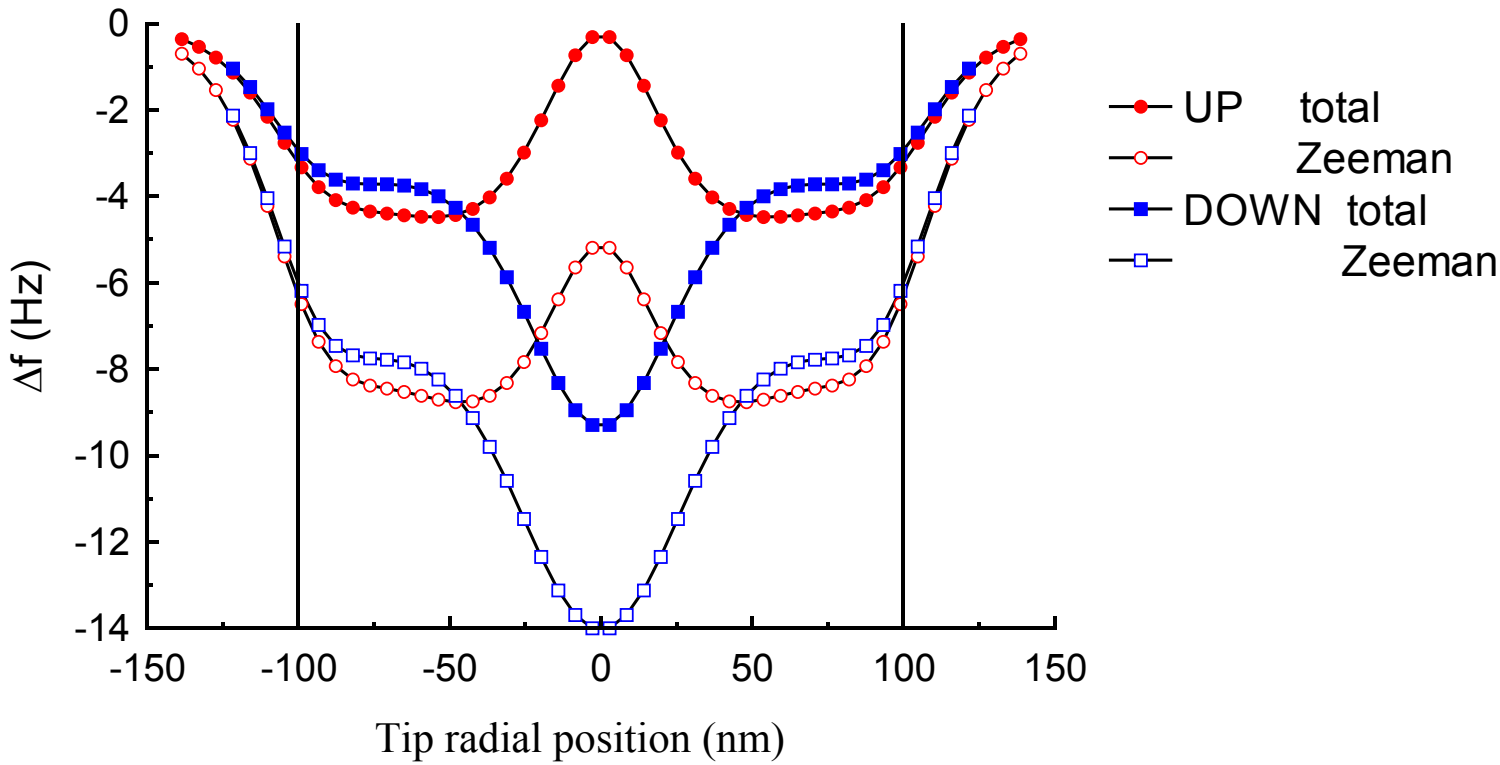

With only the interaction energy term

- twice the overall attraction, for about the same core contrast

- bigger asymmetry in core image intensity and width

Global attractive contrast vs. tip strength

Rectangular element in S state, 2.1 x 0.7 µm x 16 nm
monopole height above sample midplane 53 nm

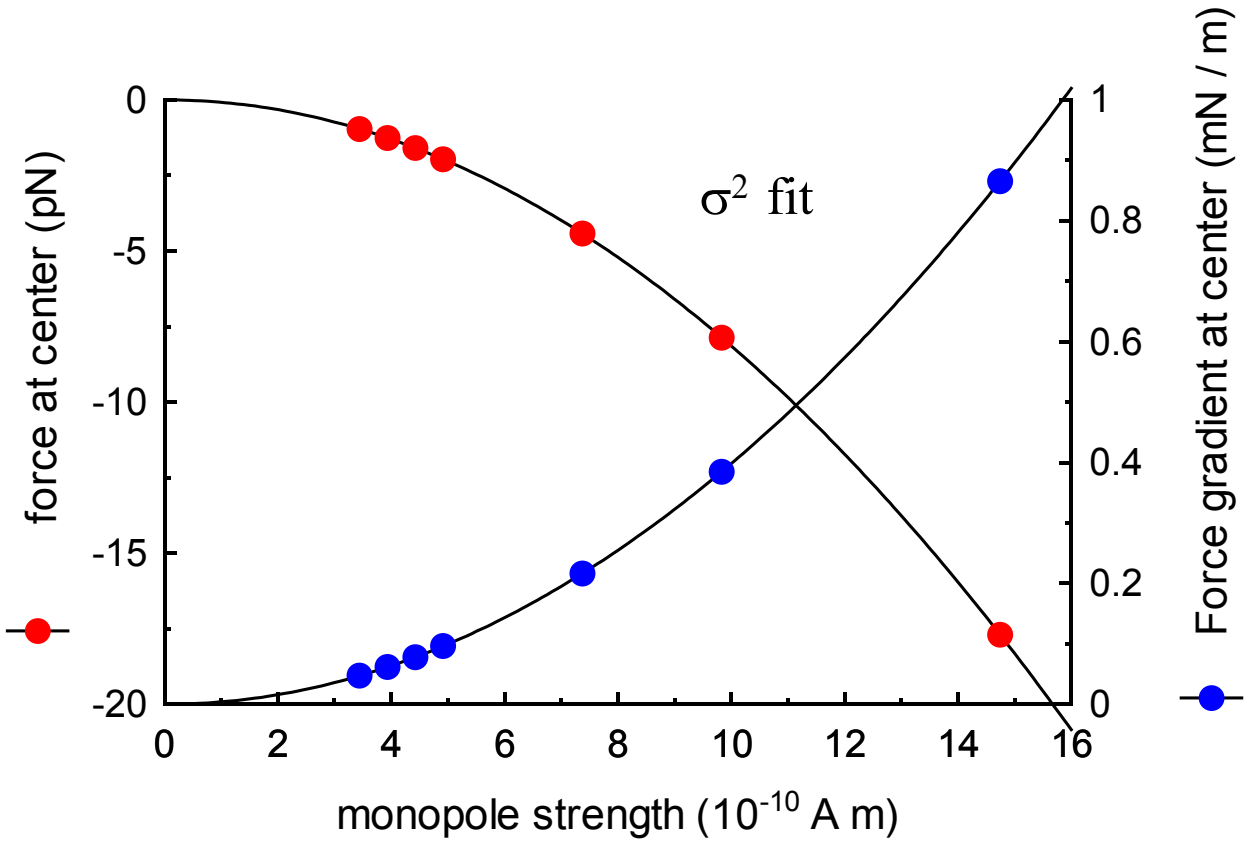

Résolution : le cas du coeur de vortex

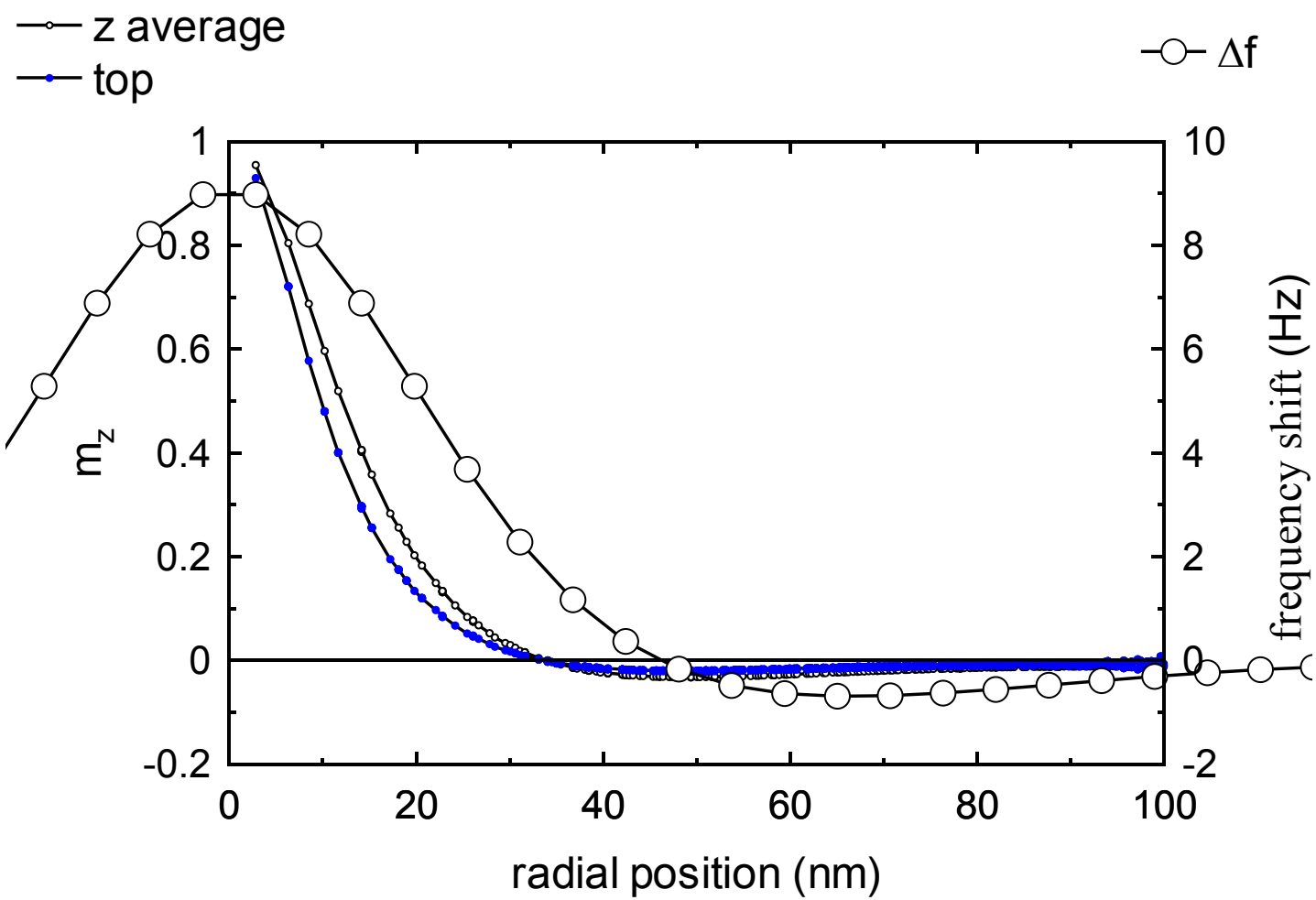

Diam 200 nm, thickness 50 nm, effective tip height above midplane 65 nm

Résolution du MFM

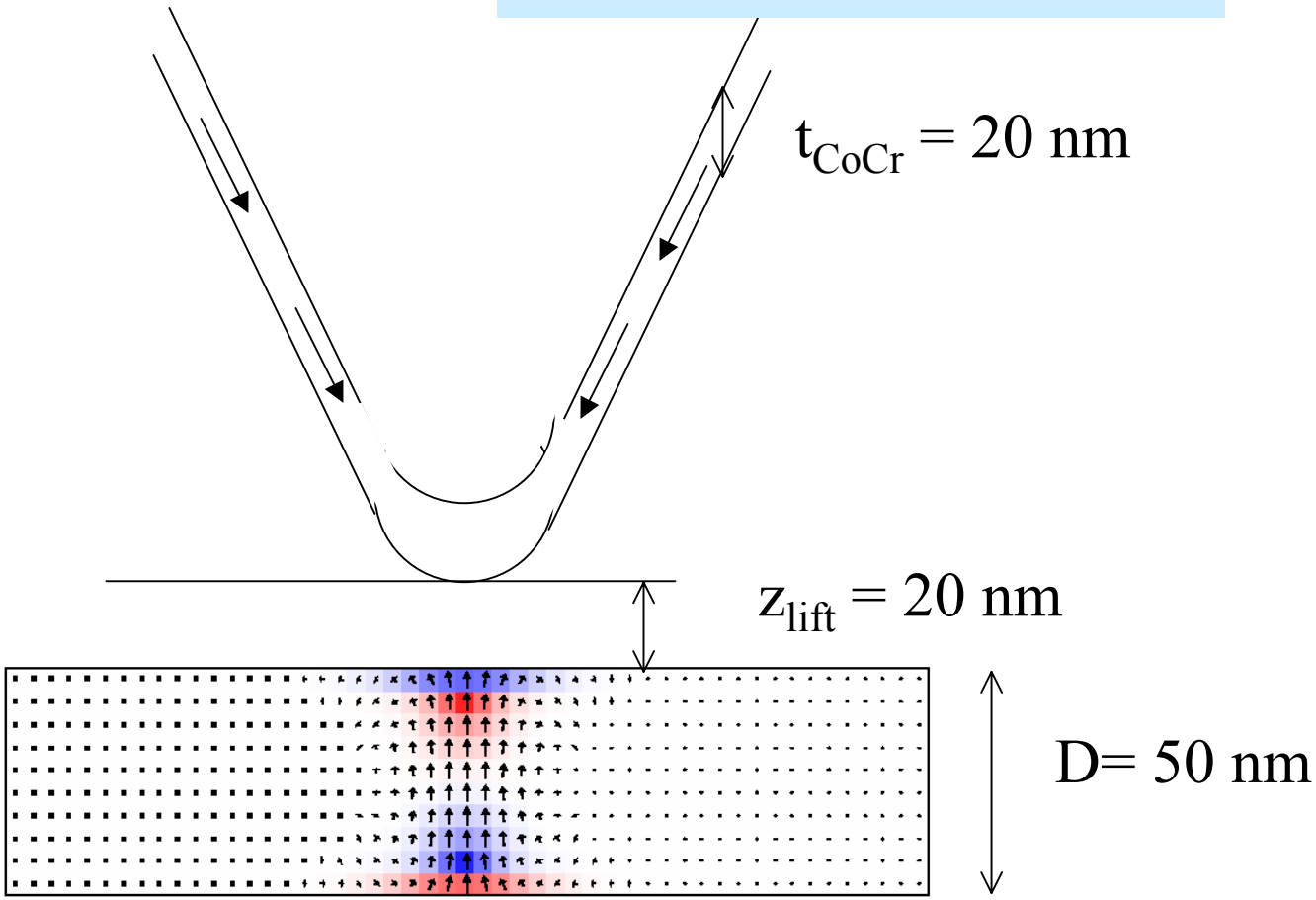

Résolution du MFM

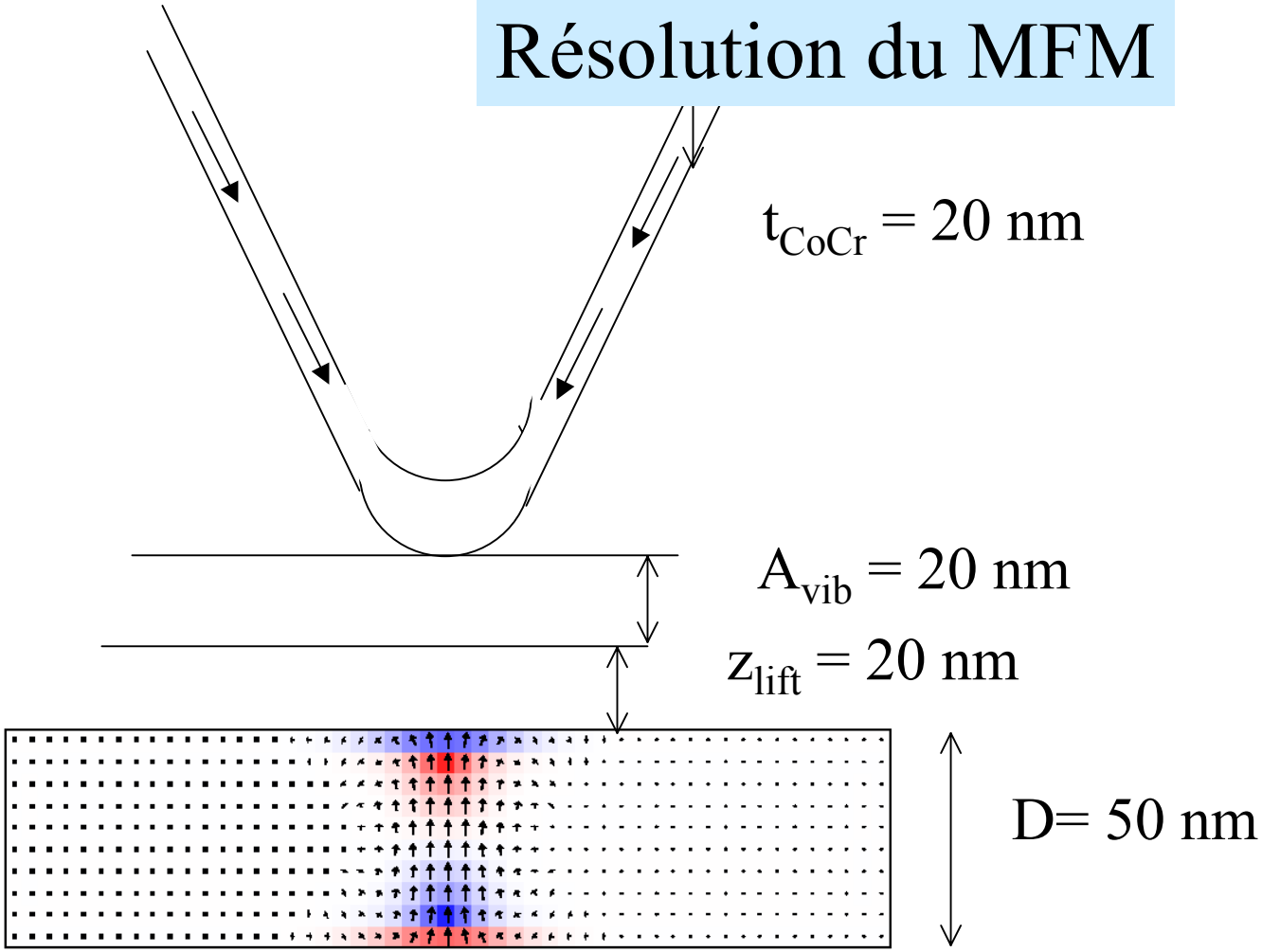

Améliorer la résolution du MFM

	perturbation	signal	bruit
réduire la couverture de la pointe	-	-	0
réduire la hauteur de vol	+	+	0
réduire l'amplitude de vibration	(-)	(-)	+
passer sous vide	0	0	-
baisser la température	(+)	(+)	-

Irreversible perturbations (1)

↔ tip-scanning direction

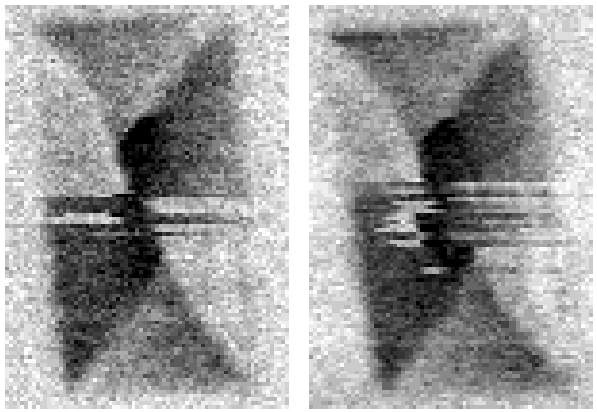

instabilities due to the vortex movement

tip-scanning direction ↕

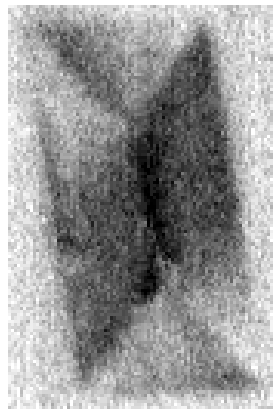

Micromagnetic Simulations

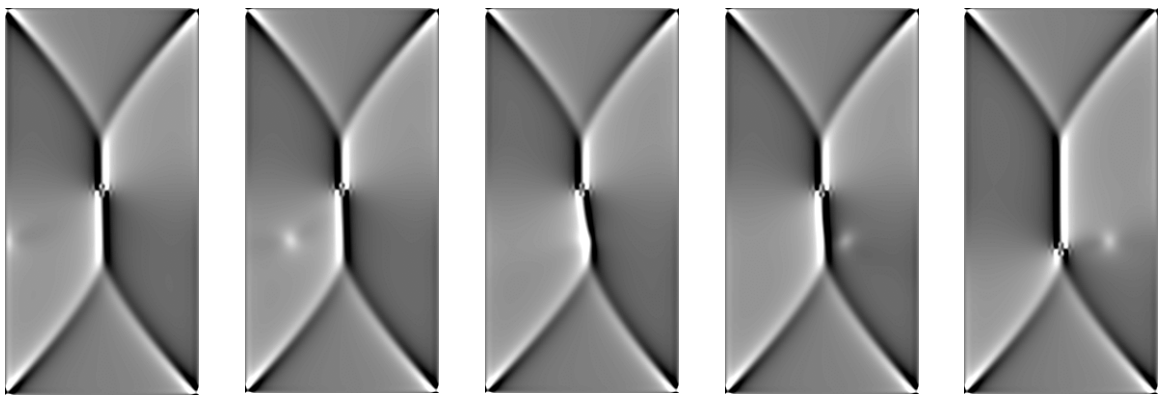

Sample magnetization distrib. for different tip locations

Parameters:

z=20 nm, z_{eff}=45 nm

σ = 9.8x10^{-10} A m, mesh=16 nm

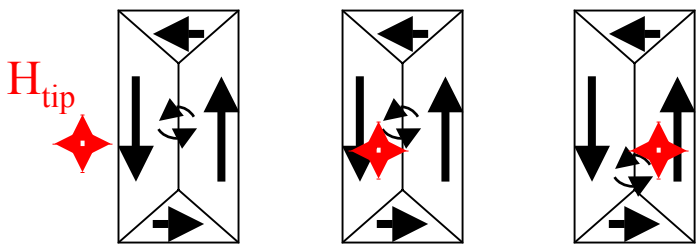

J. M. García et al., J. Magn. Magn. Mater. **242-245** (2002) 1267

Irreversible perturbations (2)

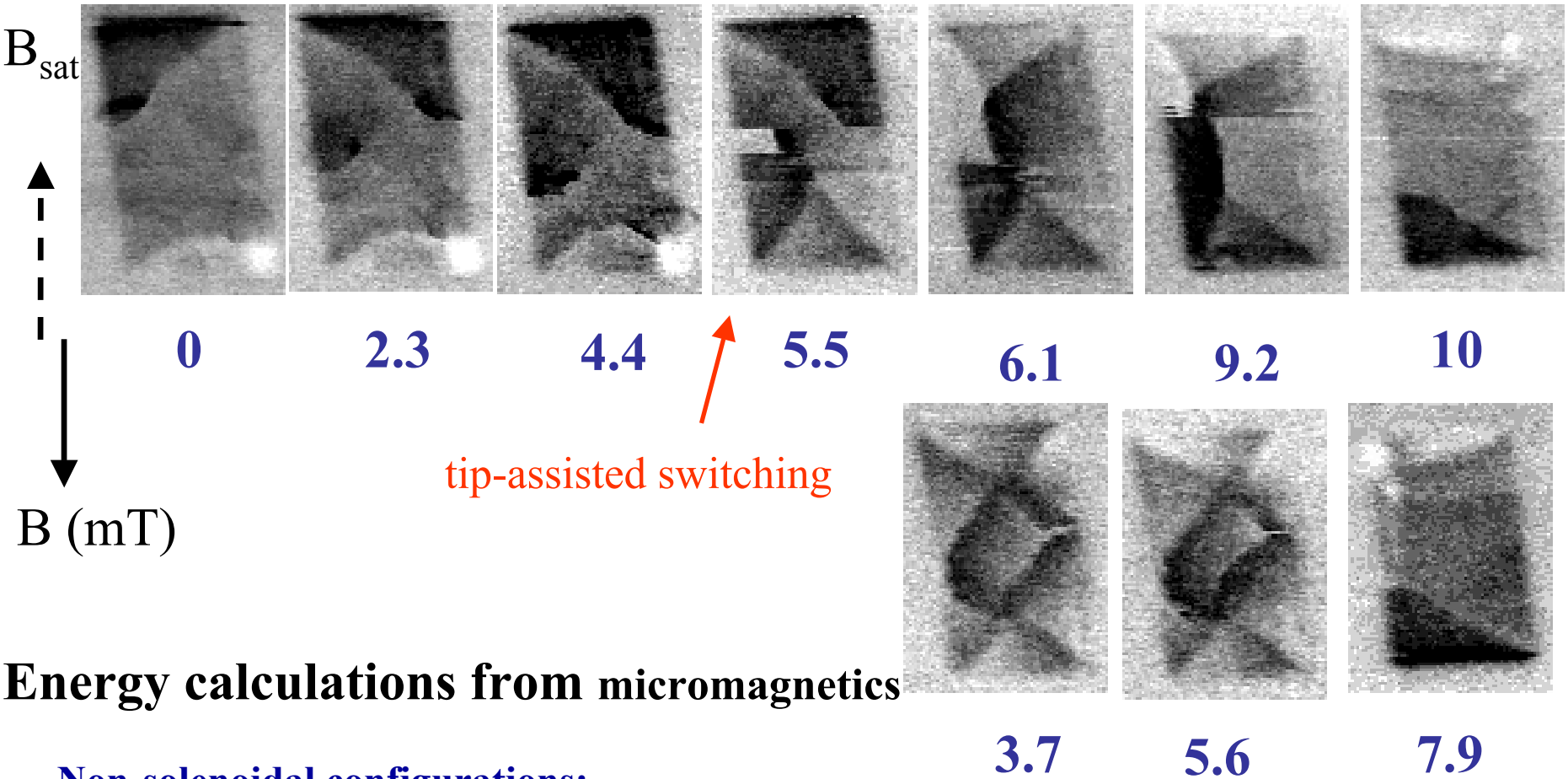

Energy calculations from micromagnetics

Non-solenoidal configurations:

C-state: E=2795 J/m^3 ; S-state: E=2798 J/m^3

Flux-closure configurations:

Diamond state: E=1310 J/m^3 ; Landau state: E=1435 J/m^3

Microscopie tunnel polarisée en spin

M. Bode, Rep. Prog. Phys. **66** 523-582 (2003)

1990 – 1992 : premières images de R. Wiesendanger (Bâle)
Cr (001), $Fe_3 0_4$ (001) pointe recouverte de CrO_2
Mode de courant constant

1998 - : images indiscutables Bode-Wiesendanger (Hambourg)
Gd(0001), Fe/W(110), Cr(001), Mn …..
Mode de spectroscopie, sur des états de surface polarisés en spin

Effet tunnel

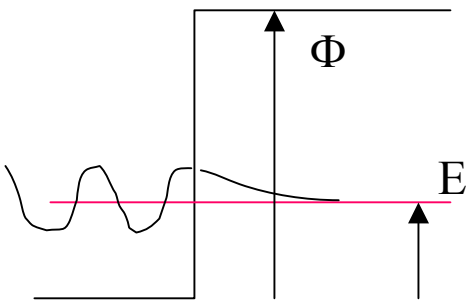

$$E = \frac{\hbar^2 k^2}{2m} \qquad E = \frac{\hbar^2 k'^2}{2m} + \Phi$$

dans la barrière

$$\Psi = e^{-iEt/\hbar} e^{-x/L}$$

$$L = \frac{\hbar}{\sqrt{2m(\Phi - E)}}$$ = 1 Å pour Φ-E= 5 eV

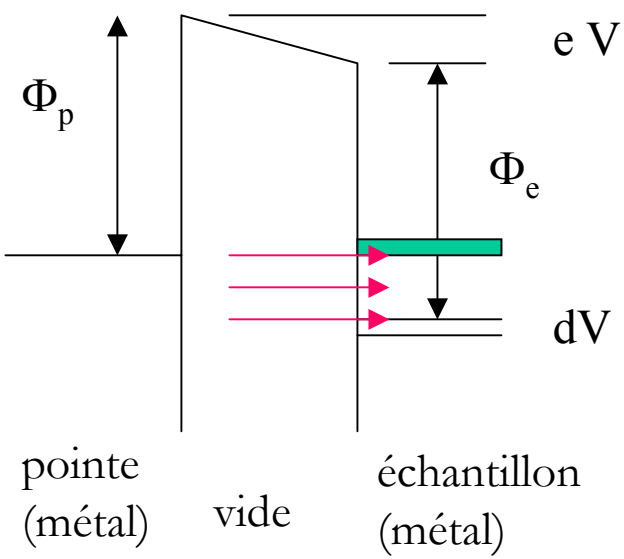

$$I = \int_{E_F}^{E_F + eV} N_{tip}(E - eV) N_{ech}(E) M \, dE$$

$$\frac{dI}{dV}(V) = eM \, N_{tip}(E_F) N_{ech}(E_F + eV)$$

Effet tunnel et spin (Jullière 1975)

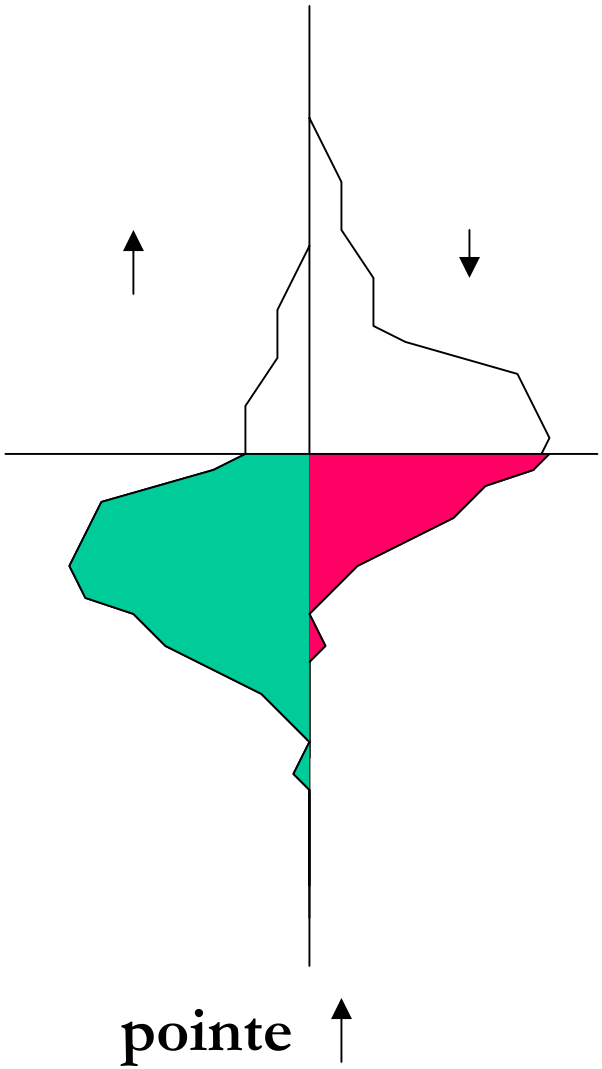

E_F

$N_pN_e + n_pn_e$

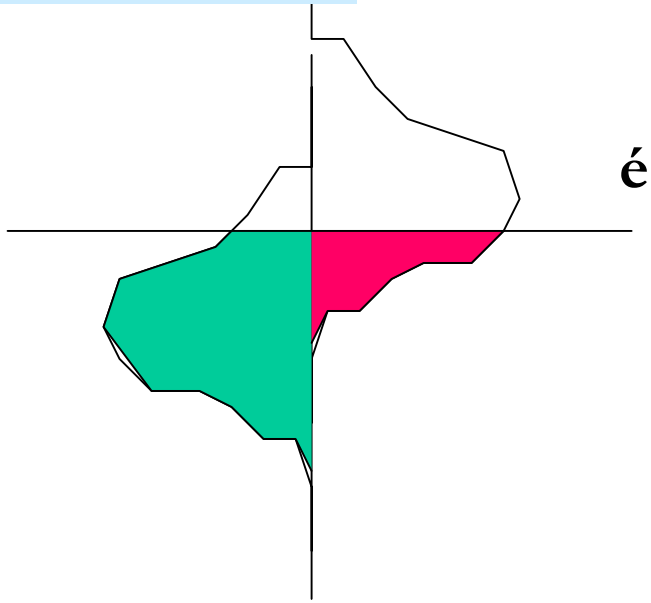

$N_pn_e + n_pN_e$

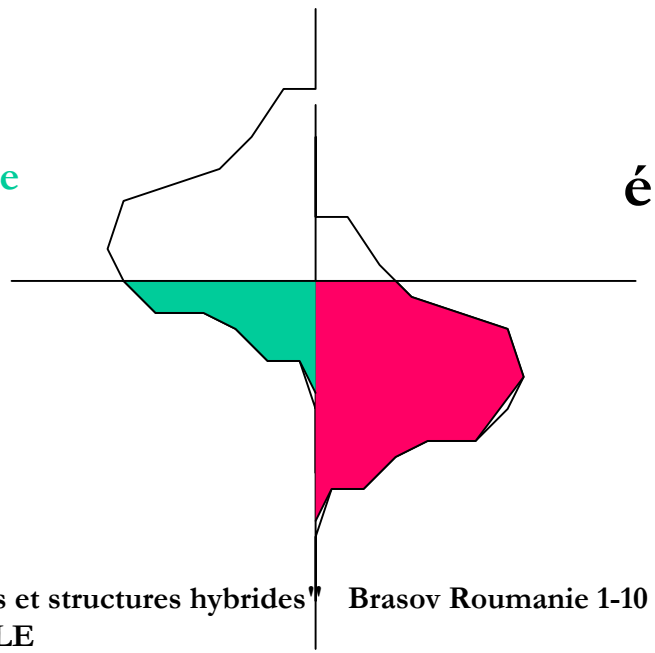

Principe

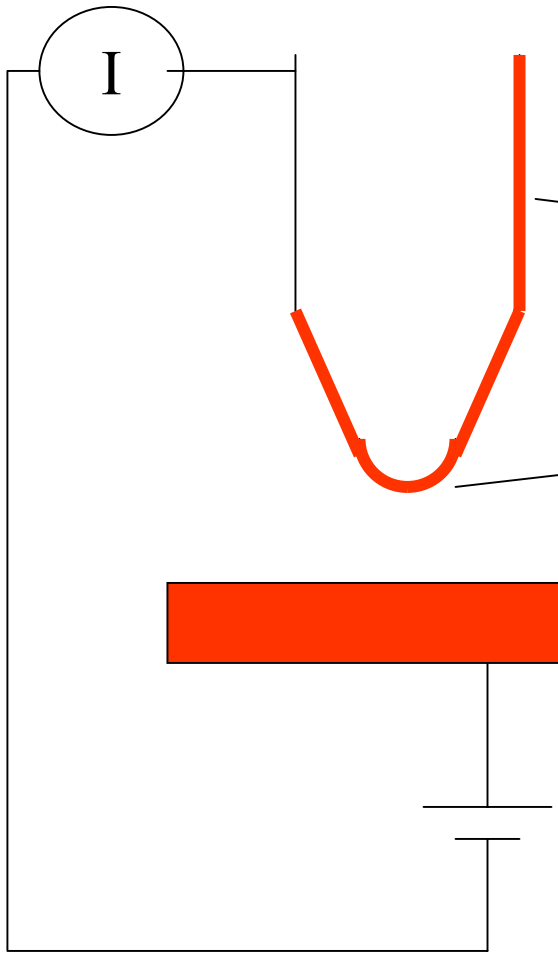

quelques monocouches
de métal magnétique
(antiferromagnétique)

configuration magnétique
contrôlée et stable

domaines assez petits et localisables

$U = U_0$ [+ $dU \cos(\omega t)$]

Pointe

W usuel + flash 2000° + dépôt magnétique

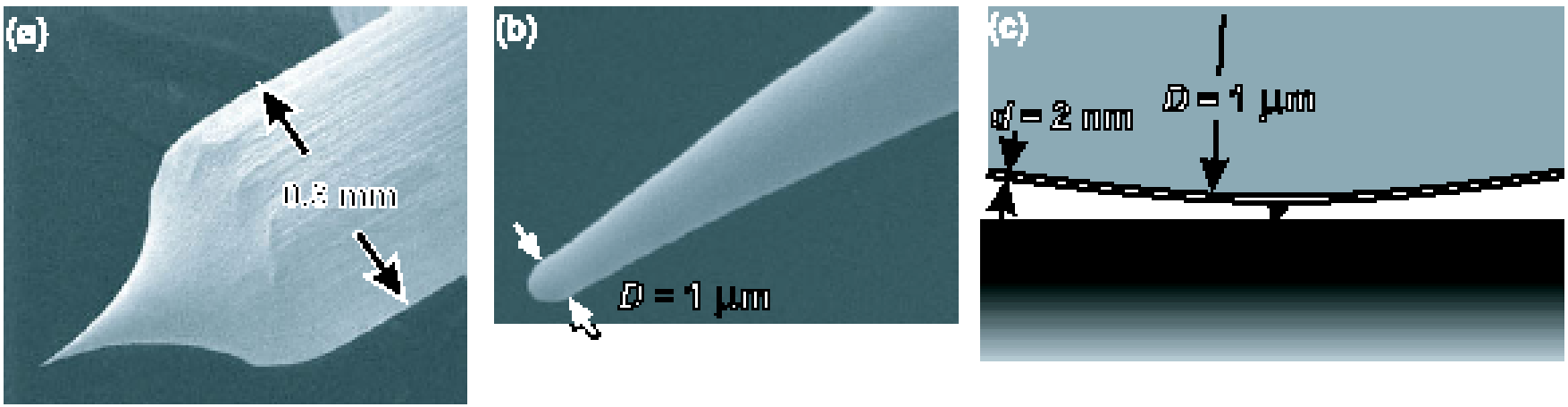

Figure 10. SEM-micrographs of an electrochemically etched, polycrystalline W tip after a high temperature flash at $T > 2200$ K. (*a*) The overview shows the shaft of the tip which exhibits a diameter of 0.8 mm. (*b*) High-resolution SEM image of the very end of the tip. The tip apex has an angle of about 15° and the tip diameter amounts to approximately 1 μm. (*c*) Schematic representation of the tip apex (in scale). The magnetic film is very thin compared to the curvature of the tip. Probably, a small magnetic cluster protrudes from the tip, which is responsible for the lateral resolution of SP-STM.

STM en mode courant constant

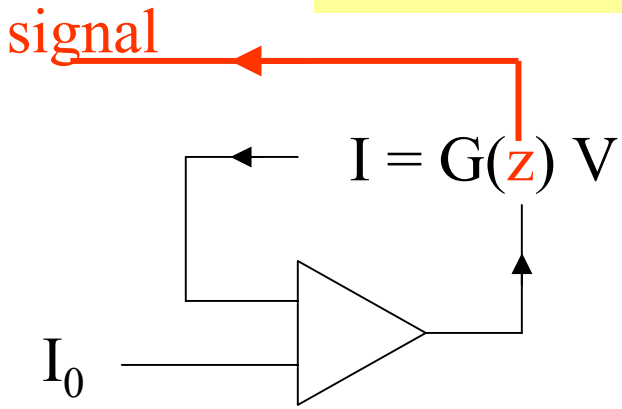

Cr(001)

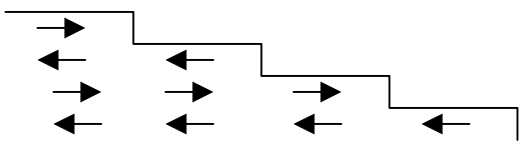

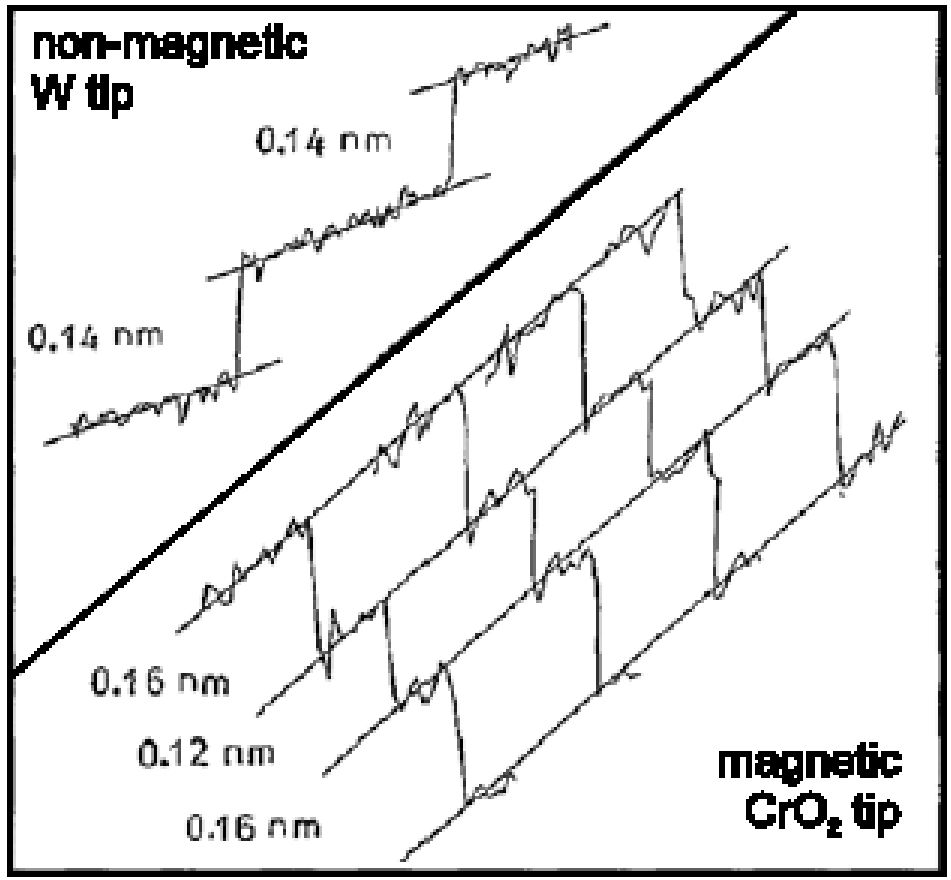

R. Wiesendanger et al.
Phys. Rev. Lett. **65** 247 (1990)

STM au travers d'états de surface polarisés en spin

(M. Bode et al., Phys. Rev. Lett 81 4256 (1998))

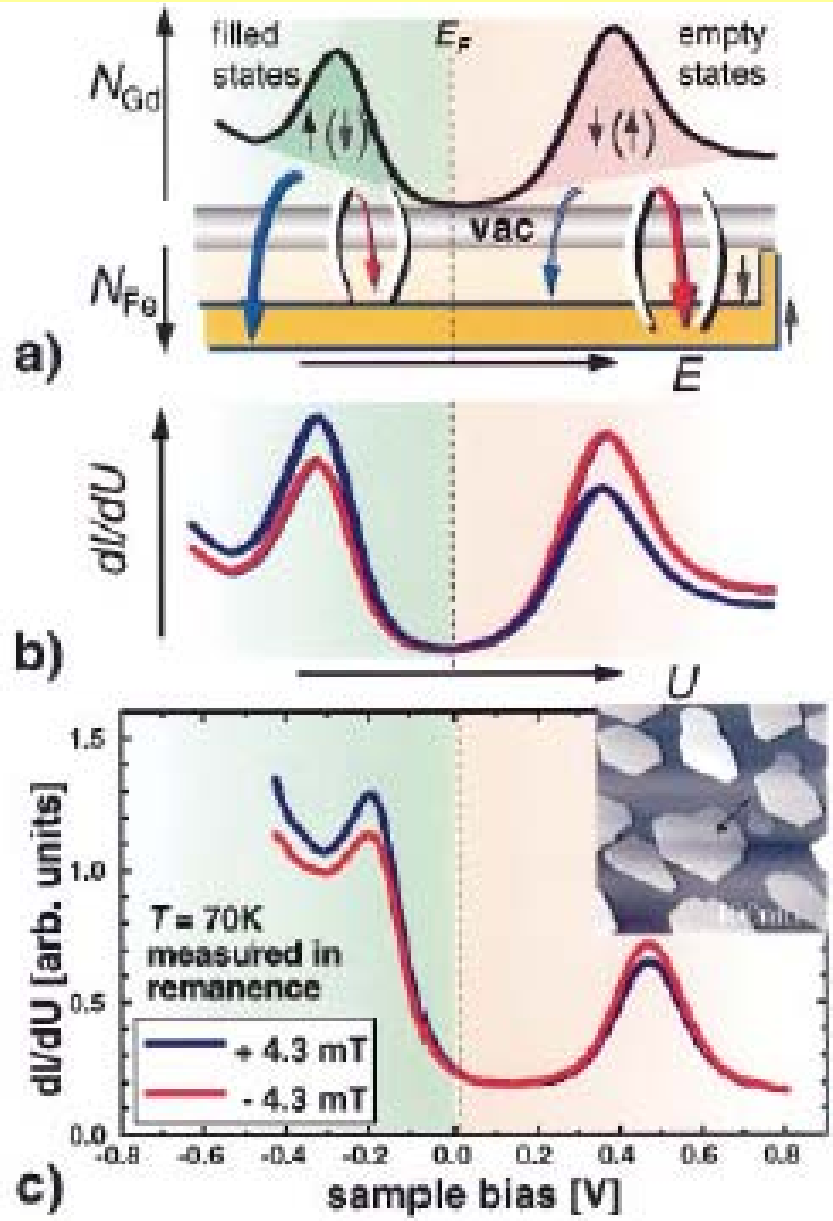

pointe : Fe 5-10 PA

éch : Gd(0001)
îlots de 20 PA

Contraste magnétique fort aux tensions correspondant aux états de surface polarisés en spin, sinon pas de contraste

STM en mode spectroscopie

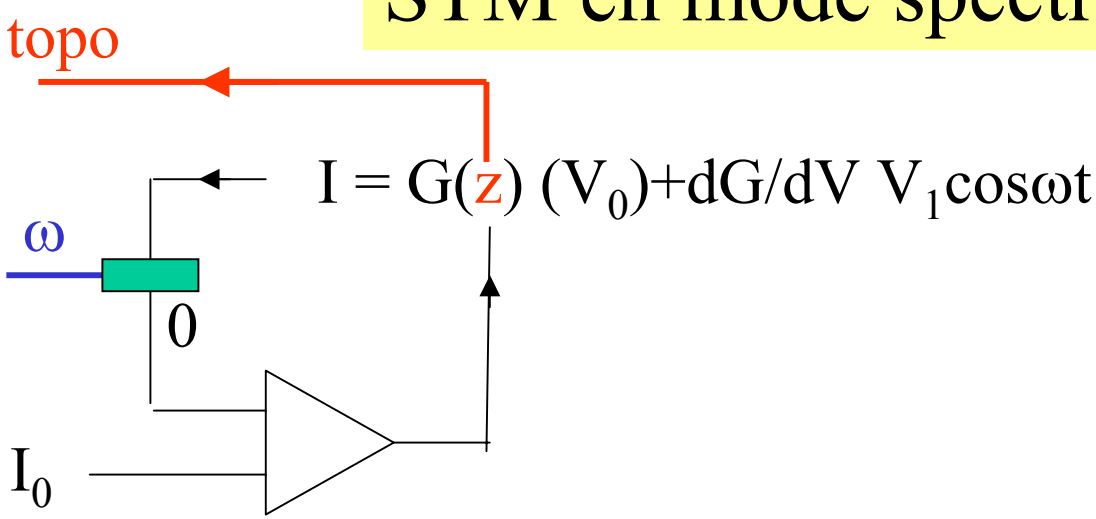

Cr(001)

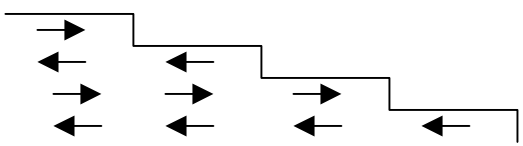

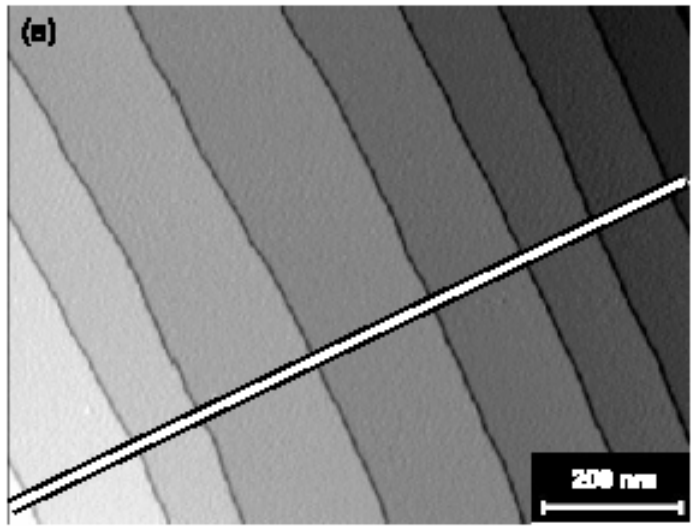

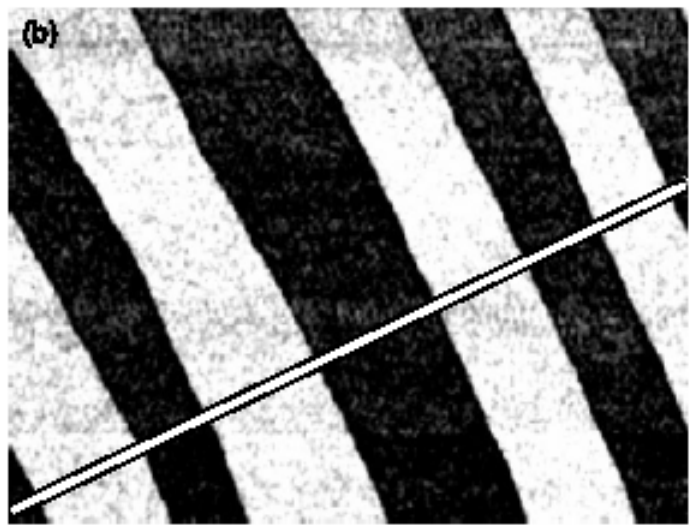

M. Kleiber et al.
Phys. Rev. Lett. **85** 4606 (2000)

U= + 0.2 V

U= - 0.45 V

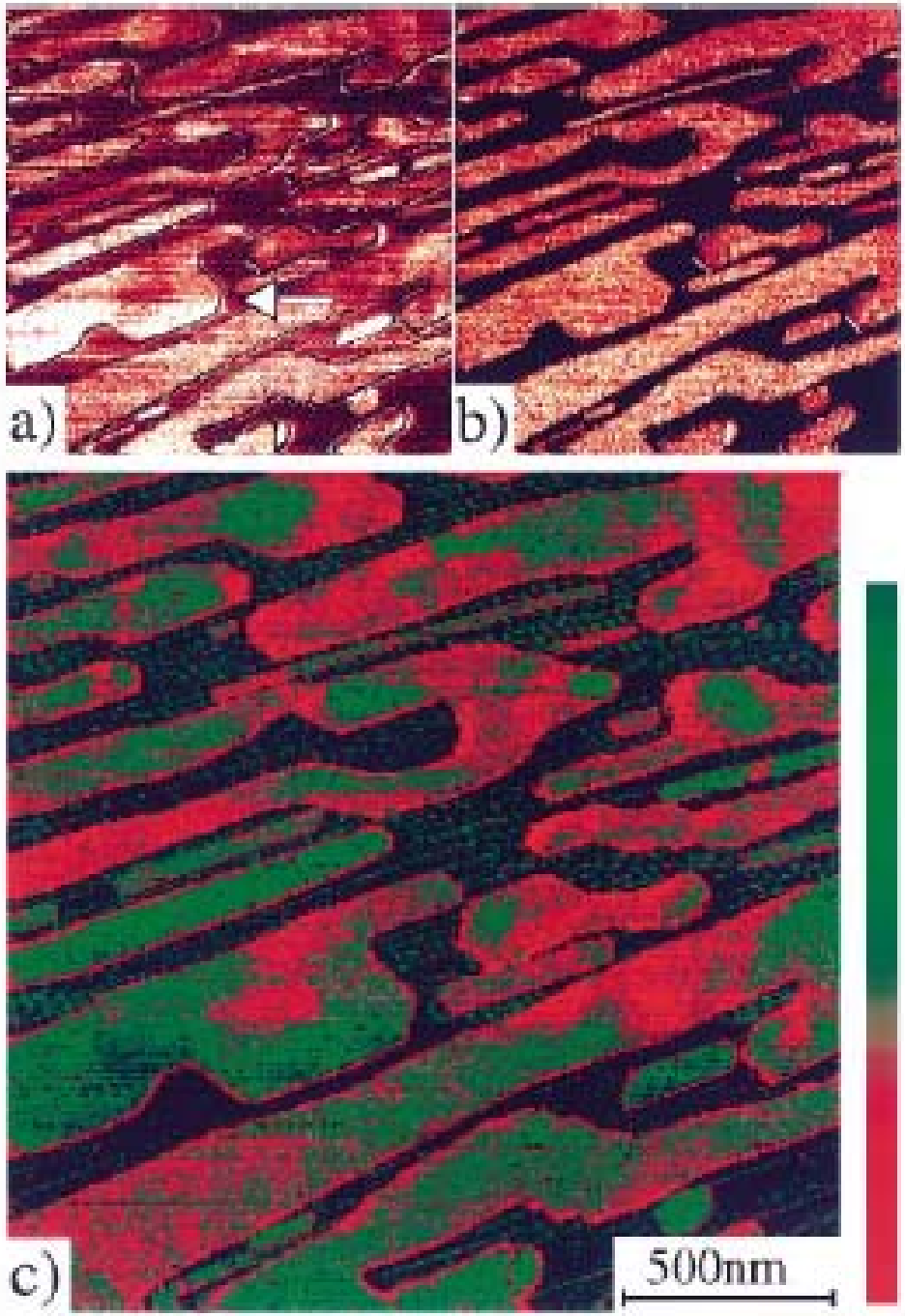

FIG. 2(color). dI/dU image at the majority (a) $U =$

L'échantillon Fe/W(110)

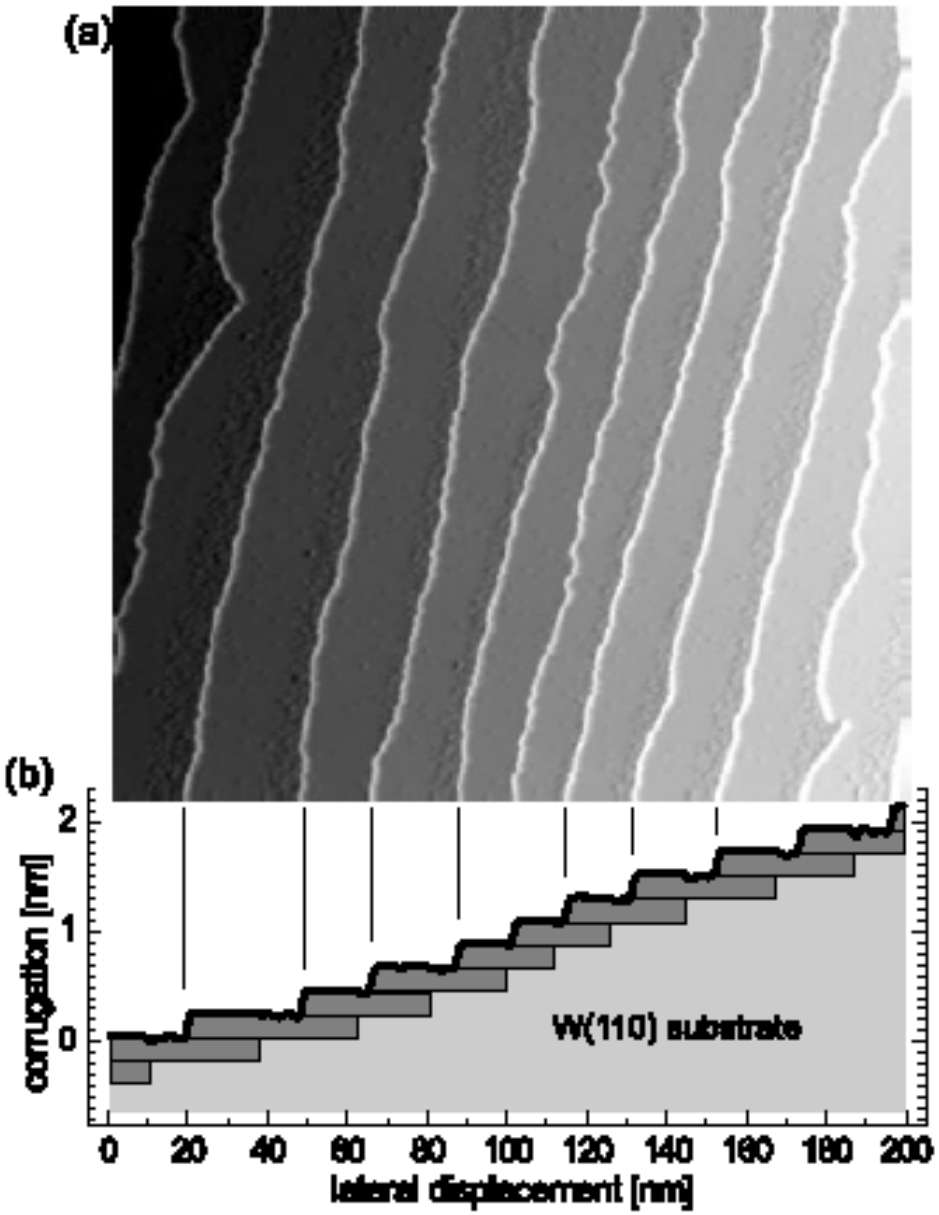

Croissance par avancée de marches à 500 K, observation à 13 K

désaccord de maille 9.4%

zone 1 PA :
pseudomorphe
aimantation plane [1-10]

zone 2 PA :
lignes de dislocations
aimantation perpendiculaire [110]

Spectroscopie sur la zone à 2 plans atomiques

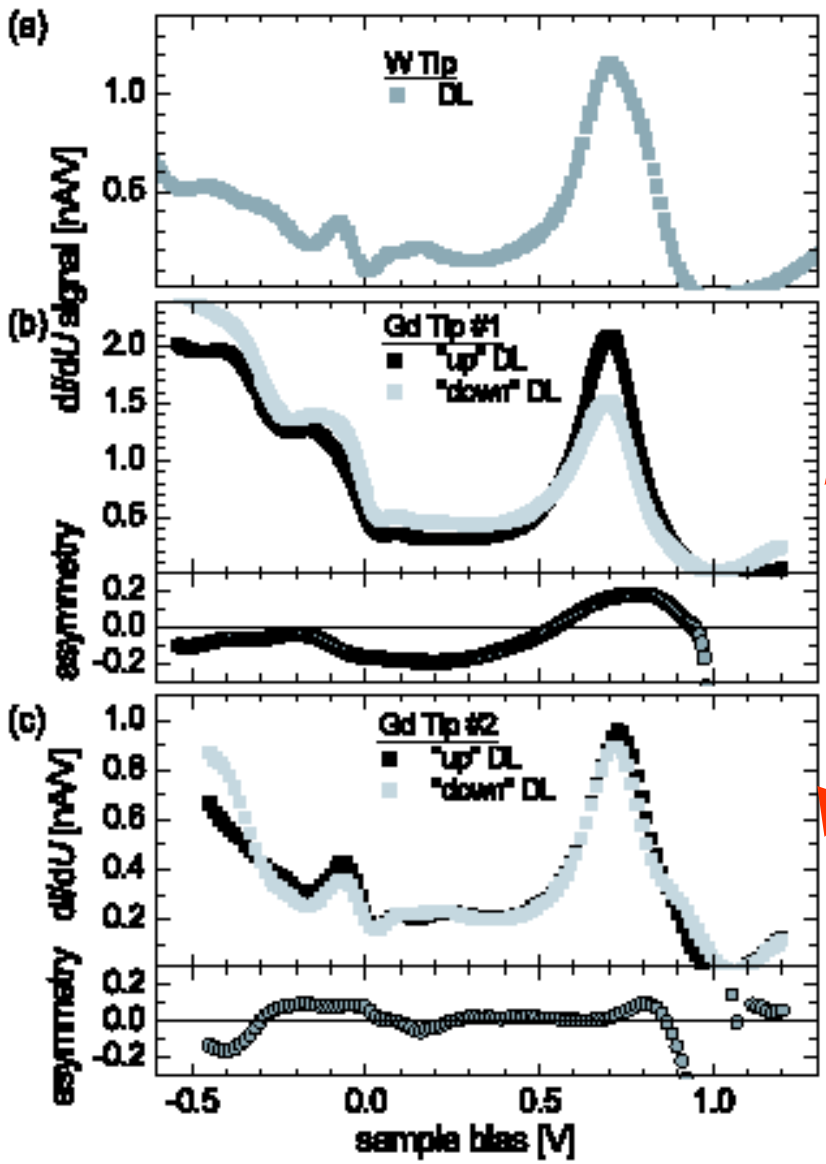

Pointe W

Deux pointes W recouvertes de Gd (sur les domaines)

Une pointe W recouverte de Fe (sur les parois)

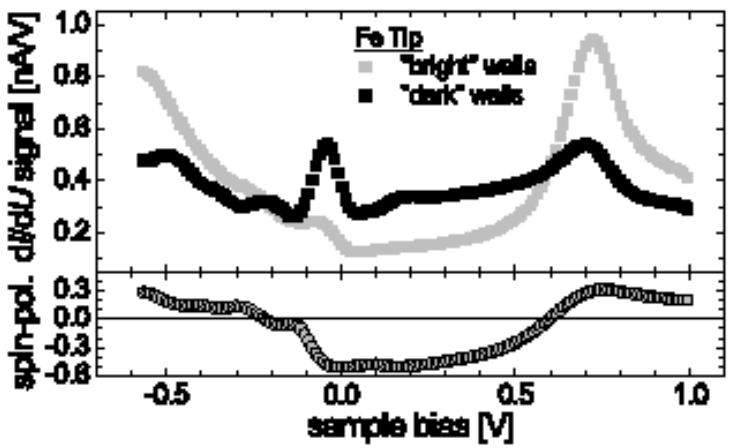

Images d'un échantillon à 2 plans atomiques

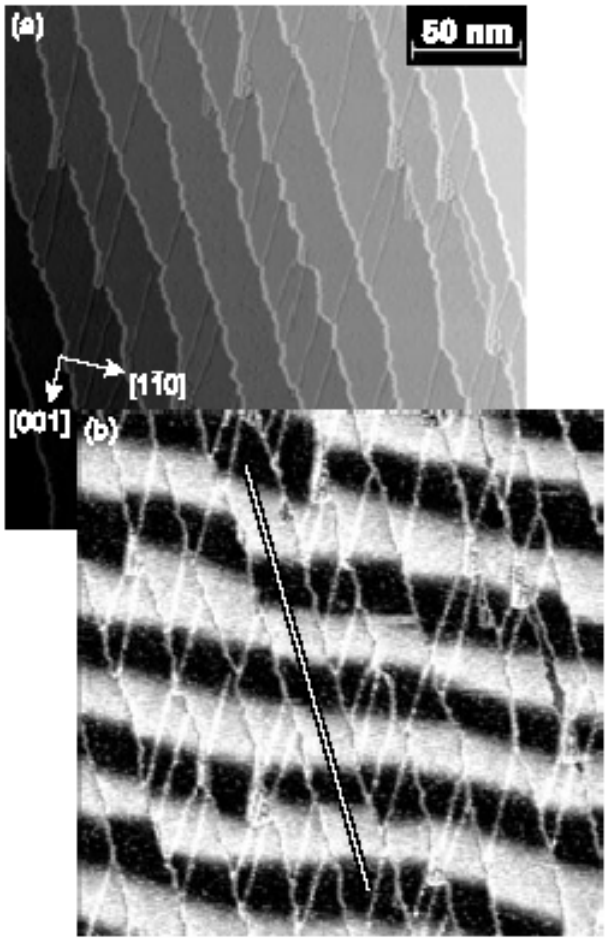

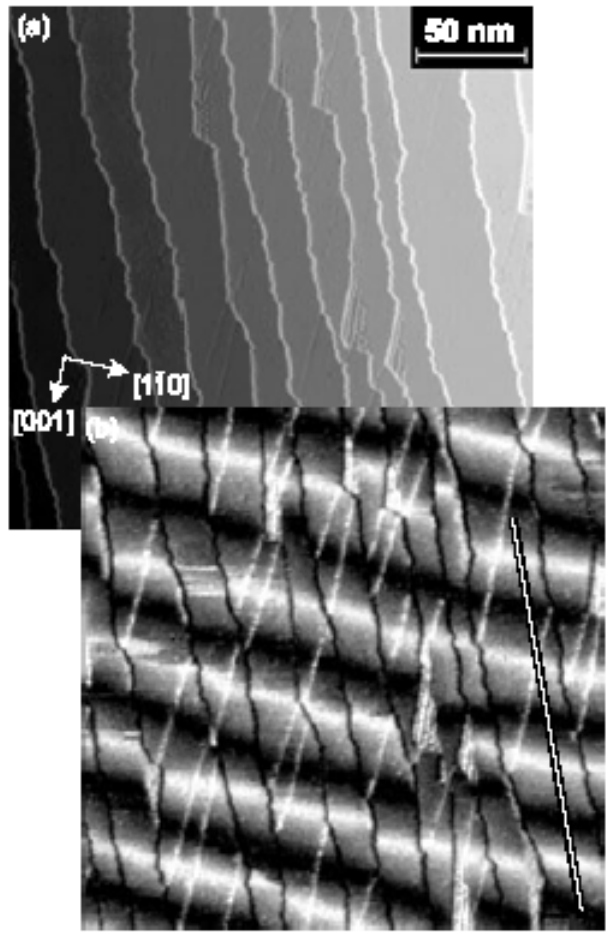

Pointe Gd, -0.45 V

domaines

Pointe Fe, -0.3 V

parois

échantillon à 1.25 plans atomiques

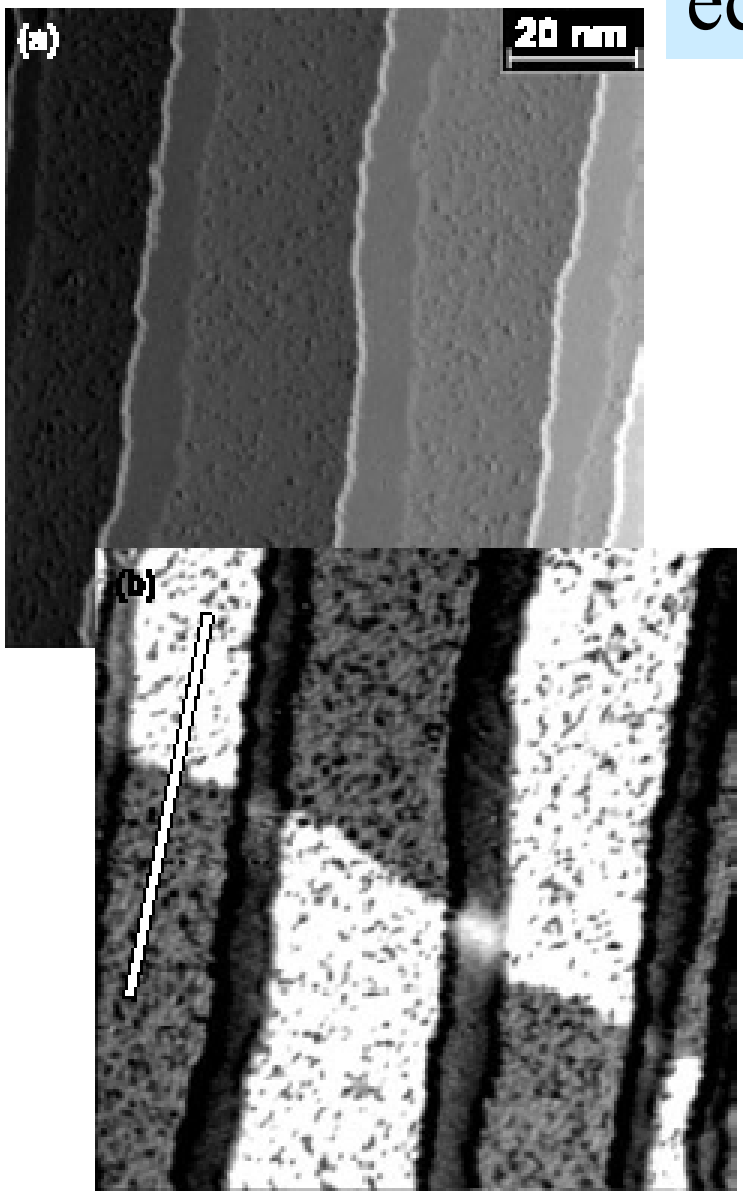

I= 0.8 nA U=+130 mV
W tip coated by 5-10 ML Fe

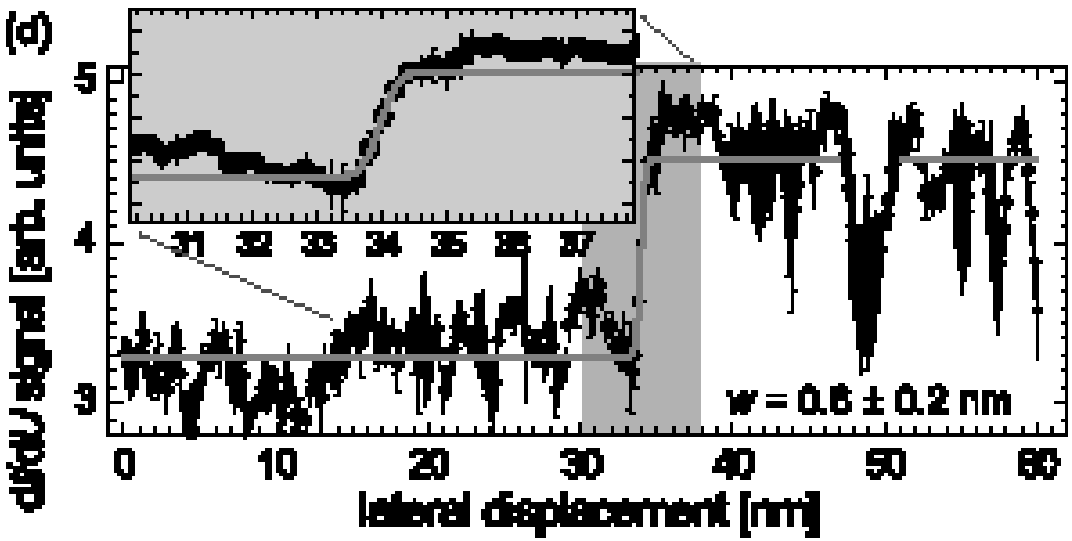

M. Pratzer et al.
Phys. Rev. Lett. **87**, 127201 (2001)

Tailles des parois

échantillon 2PA

mesure SP-STM : $2\Delta = 7.3 +/- 0.5$ nm

$K = 10^6$ J/m^3 (Elmers 1999)

$A = A_{massif} = 10^{-11}$ J/m → $2\Delta = 6.3$ nm

échantillon 1PA

mesure SP-STM : $2\Delta = 0.6$ nm

$K = 40\ 10^6$ J/m^3

$A = 0.4\ 10^{-11}$ J/m

estimés

Imagerie d'un vortex par SP-STM

(A. Wachowiak et al., Science **298** 577 (2002))

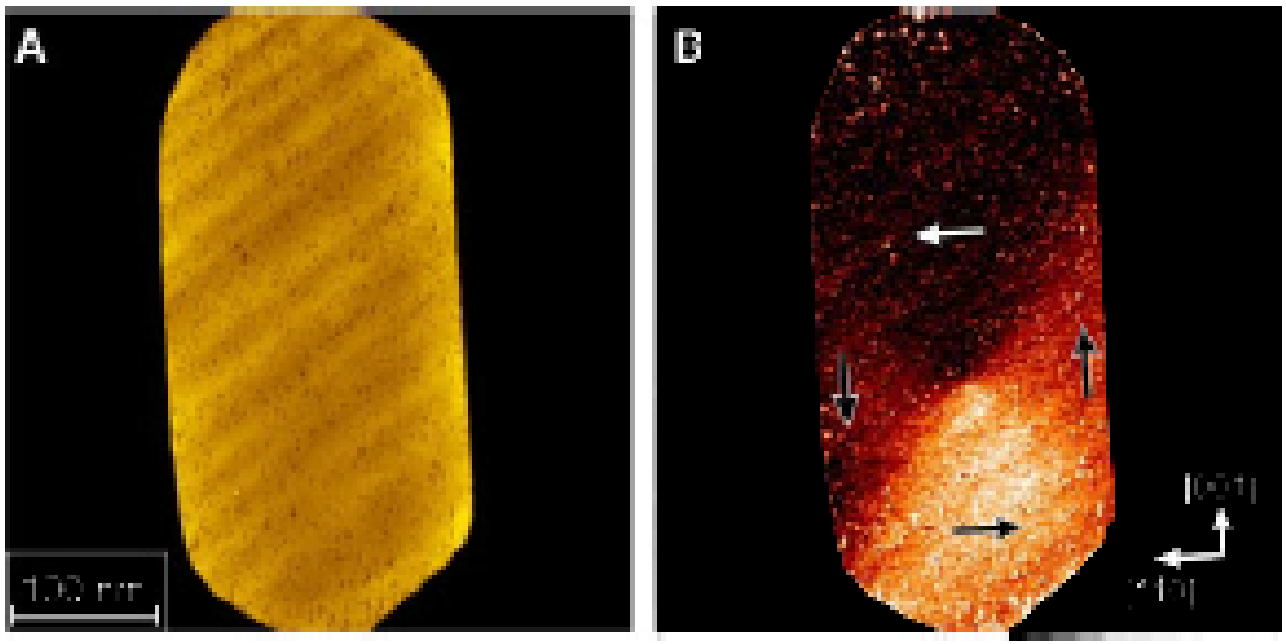

Fig. 2. (A) Topography and (B) map of the dI/dU signal of a single 8-nm-high Fe island recorded with a Cr-coated W tip. The vortex domain pattern can be recognized in (B). Arrows illustrate the orientation of the domains. Because the sign of the spin polarization and the magnetization of the tip is unknown, the sense of vortex rotation could also be reversed. The measurement parameters were $I = 0.5$ nA and $U_0 = +100$ mV. The crystallographic orientations were determined by low-energy electron diffraction.

in plane perpendicular

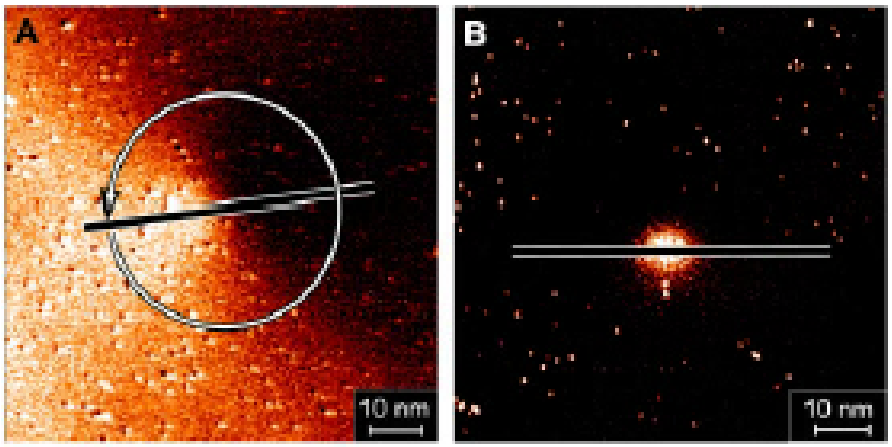

Fig. 3. Magnetic dI/dU maps as measured with an (A) in-plane and an (B) out-of-plane sensitive Cr tip. The curling in-plane magnetization around the vortex core is recognizable in (A), and the perpendicular magnetization of the vortex core is visible as a bright area in (B). (C) dI/dU signal around the vortex core at a distance of 19 nm [circle in (A)]. (D) dI/dU signal along the lines in (A) and (B). The measurement parameters were (A) $I = 0.6$ nA, $U_0 = -300$ mV and (B) $I = 1.0$ nA, $U_0 = -350$ mV.

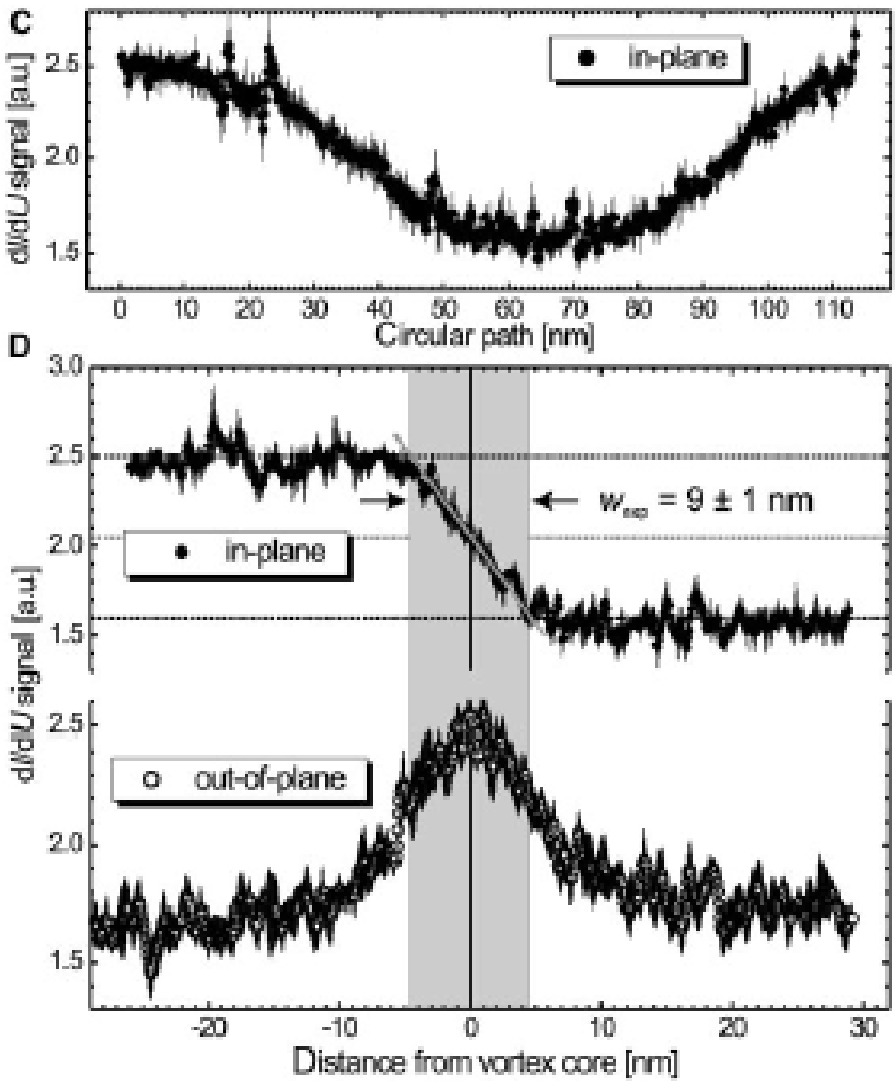

théorie 2d : $w = 2.64\ \Lambda$

Fig. 4. dI/dU maps measured with an out-of-plane sensitive Cr tip at (A) zero field and (B) a perpendicular field $\mu_0 H_{ext} = -800$ mT. The inset shows the vortex core at the position it is found at $\mu_0 H_{ext} = +800$ mT. The measurement parameters were $I = 0.5$ nA and $U_0 = -0.3$ V. (C) Experimental (lines) and calculated data of the perpendicular magnetization of the vortex core at (●) zero field, (Δ) $\mu_0 H_{ext} = +800$ mT, and (∇) $\mu_0 H_{ext} = -800$ mT. (D) Magnified representation of the zero field data in (C). At a distance of ≈ 18 nm, both experimental and calculated data show a weak magnetization opposite to the magnetization in the vortex core.

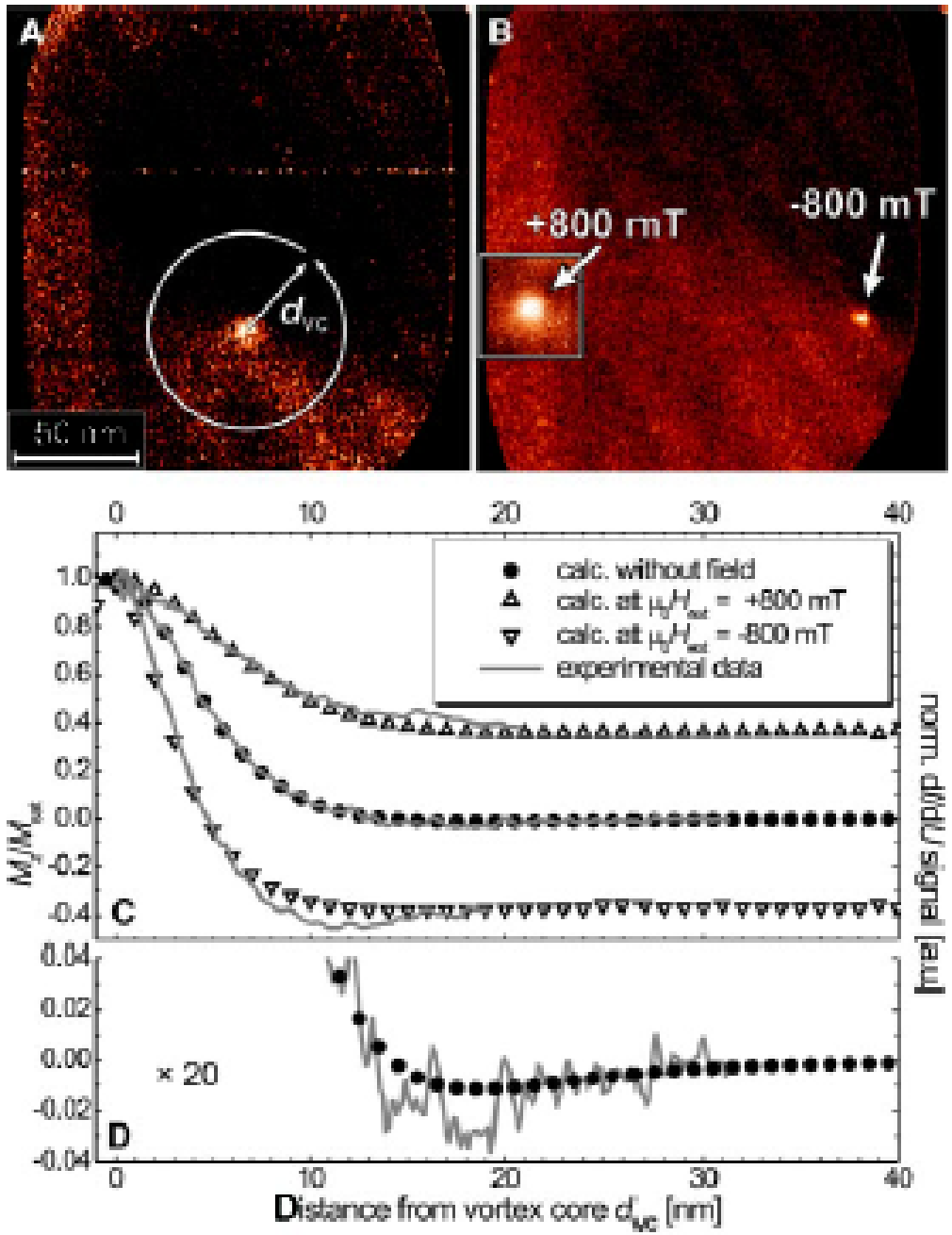

La même pointe donne 2 directions d'aimantation !

Pointe W à 5 PA de Fe
échantillon à ~1.7 PA de Fe

Topographie | dI/dU | U=-0.1 V | dI/dU | U=+0.1 V

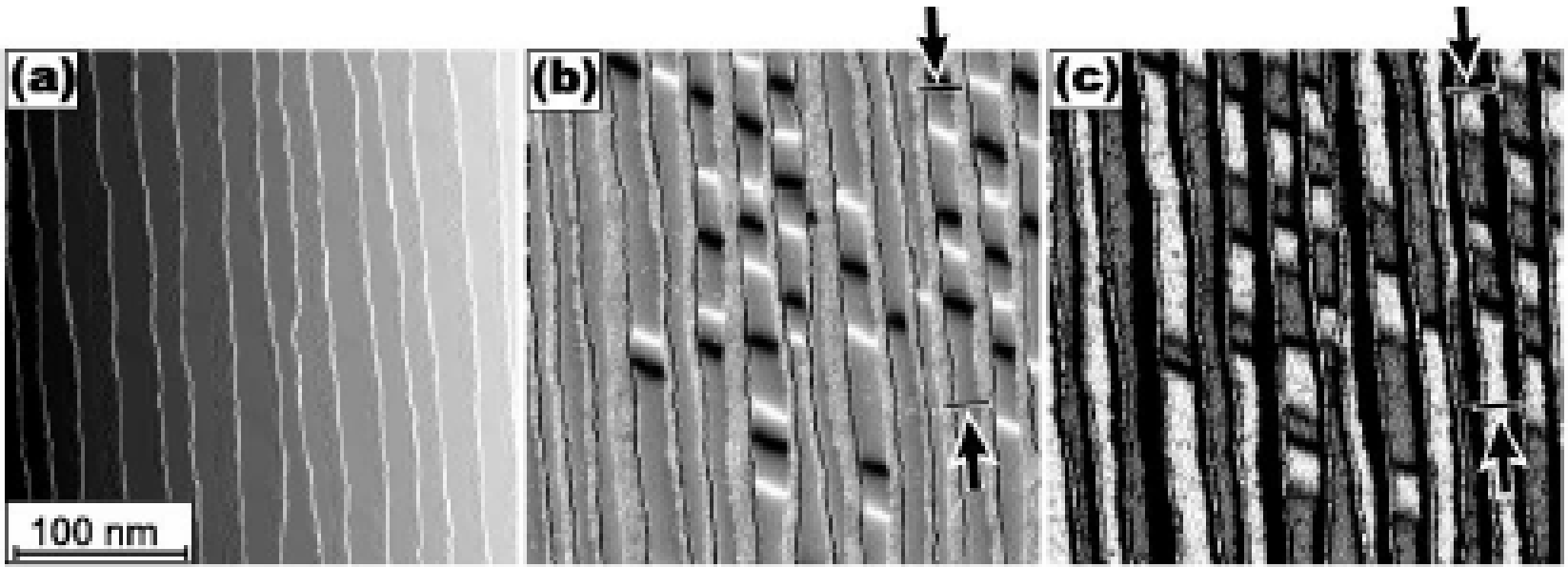

dans le plan | perpendiculaire

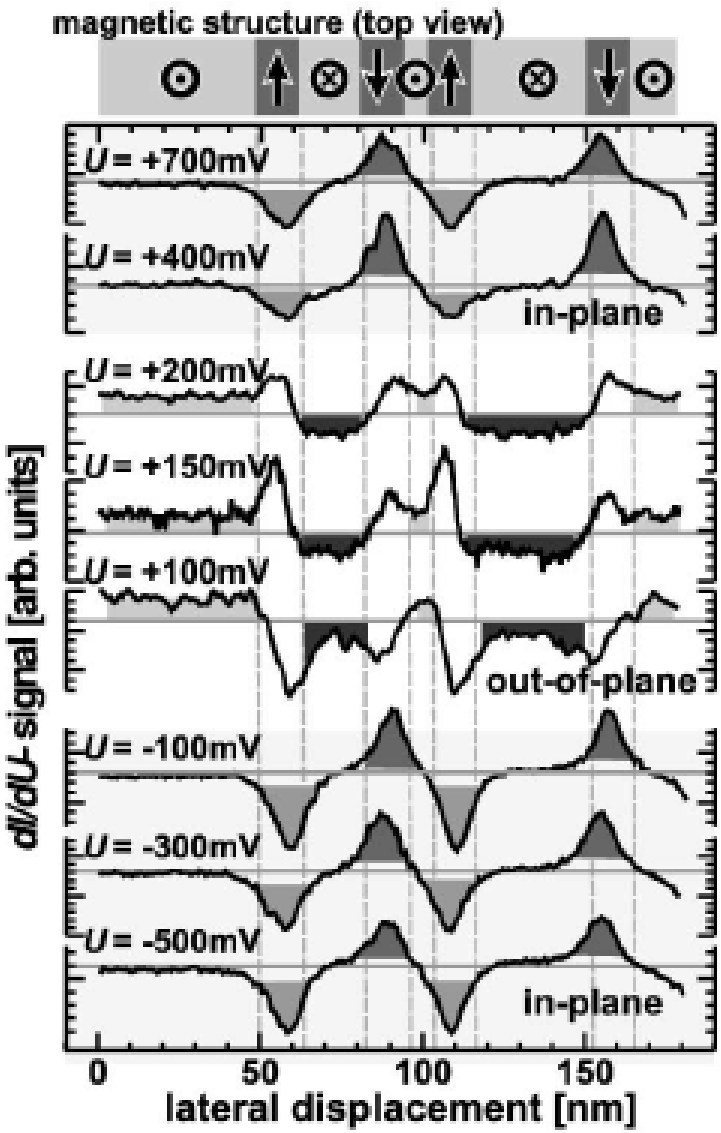

Explication avancée :
passage par différentes orbitales (de différente symétrie) portant des moments orthogonaux

M. Bode et al.
Phys. Rev. Lett. **86** 2142 (2001)

Microscopie tunnel polarisée en spin par modulation de l'aimantation de la pointe

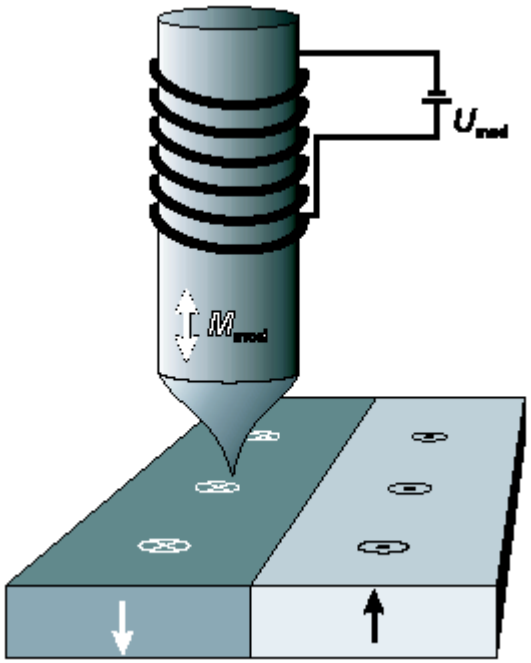

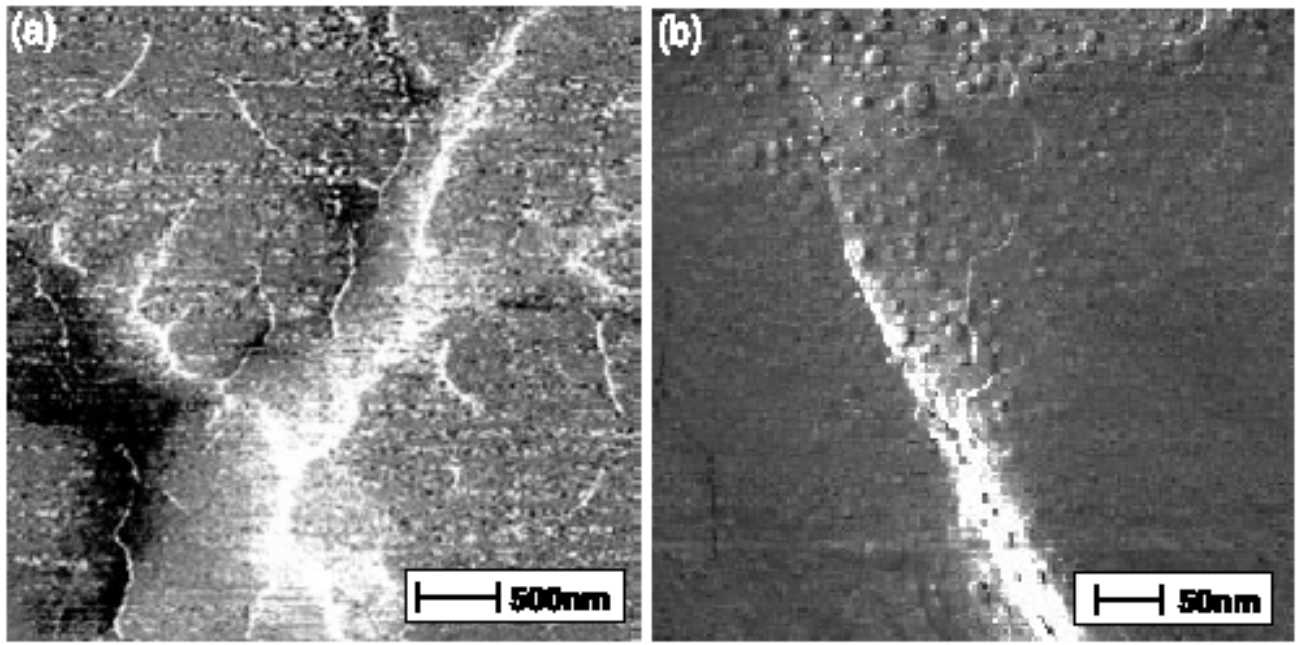

Co (0001)

W. Wulfhekel, J. Kirschner, Appl. Phys. Lett. **75** 1944 (1999)
H.F. Ding, W. Wulfhekel, J. Kirschner, Europhys. Lett. **57** 100 (2002)

Microscopie tunnel à électrons balistiques (BEEM)

W.H. Rippard, R.A. Buhrman
Appl. Phys. Lett. 75 1001 (1999)

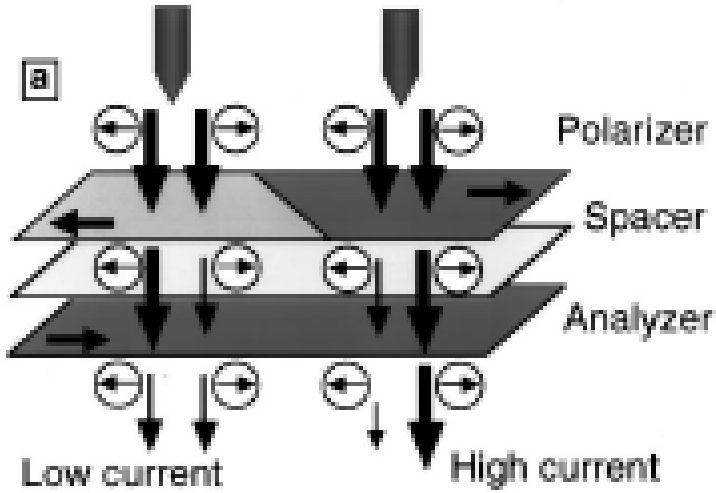

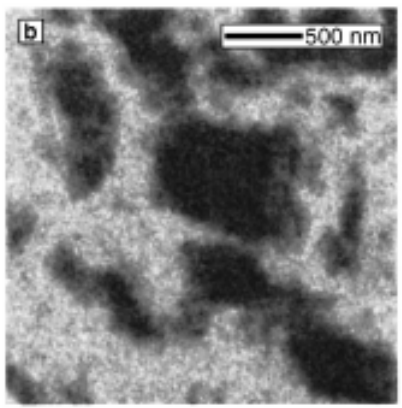

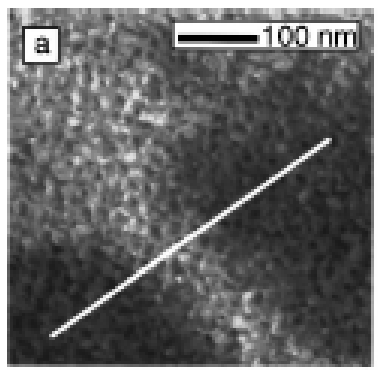

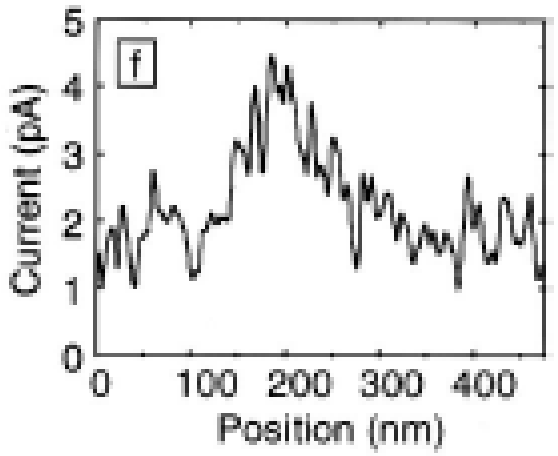

FIG. 1. (a) Schematic diagram of the "analyzer–polarizer" geometry showing how magnetic contrast is obtained in a ferromagnetic–normal-metal–ferromagnetic system. (b) Large-area ($2.5\times2.5\ \mu m^2$) scan taken after the sample has been biased into the coercive state with an applied magnetic field and the field then removed. The collector current is represented in a linear gray-scale with a range from 1.0 pA (black) to 5.0 pA (white), the background has been subtracted to enhance visual contrast. $V_t = -1.5$ V and $I_t = -2$ nA.